PHYSICAL REVIEW
LETTERS

VOLUME 7 NOVEMBER 1, 1961 NUMBER 9

DRAG FORCES IN ROTATING He II†

Paul P. Craig
Los Alamos Scientific Laboratory, University of California, Los Alamos, New Mexico
(Received September 25, 1961)

Despite many measurements on the bulk properties of rotating He II, the first local probing of the velocity field occurred only in 1960 when Pellam[1] studied the torque on a Rayleigh disk immersed in a rotating cylinder filled with He II as a function of disk position and of temperature. The most surprising result of his study occurred in the torque versus temperature measurements, which seemed to indicate that only the superfluid component of He II exerted torque upon the system, so that just below the lambda transition the torque vanished entirely. This result appears to be in conflict with all theories of He II, and provided the motivation for the present study in which the velocity field was studied in a rotating system using a different type of detector, which measures the drag forces exerted on disks placed normal to the stream lines of the rotating helium.

The detectors consisted of pairs of glass disks mounted on quartz crossbeams and suspended inside a rotating cylinder (inside diameter 5.3 cm) by means of quartz fibers fixed at their upper ends in the laboratory coordinate system. The rotating cylinder was contained in a partially silvered glass Dewar. The bottom of the rotating cylinder was sealed by a brass plate, the only connection to the main helium bath being through two 0.005-in. filling holes drilled in the plate about 0.5 mm off axis. The temperature was determined from the helium vapor pressure in the cylinder (scale $T55_E$), thereby assuring that no errors were introduced from flowing He gas. Drag forces on the disks resulted in deflection of the detectors through angles which could be measured by means of a light beam reflected from a mirror mounted on the detector, and thence onto a circular translucent scale 28 cm from the axis of rotation. A range of reproducible angular rotational velocities from 0.21 to 6 rpm was produced by a synchronous motor coupled to speed reduction gear boxes and to a lathe gear box. A leather belt decoupled the drive from the experimental Dewar, thereby reducing vibration to a negligible level.

Two detector assemblies were used. In assembly I the detectors were 1.2 cm in diameter and 0.2 mm thick. They were mounted on a diameter at 2.5 cm center-to-center separation, and suspended from a quartz fiber of torsion constant 8×10^{-2} dyne cm/rad. In assembly II the detectors were 0.6 cm in diameter and 0.2 mm thick, mounted at a center-to-center separation of 2.3 cm. The torsion constant was 4.7×10^{-3} dyne cm/rad. The fiber constants were determined from the observed deflections in air at 300°K at low Reynolds numbers where Stokes' law obtains, so that the drag forces were linear in velocity.[2] The constants obtained in this way were in reasonable agreement with those found by timing the fibers as torsion pendula using a known moment of inertia. An additional advantage of the air calibration procedure is that errors arising from the finite size of the disks tend to cancel when deflections in air are compared to those in helium. System I was additionally calibrated in CS_2 and in liquid N_2. System II was calibrated in He gas at 75°K and 580 mm Hg and at 2°K and 23.7 mm Hg as well as in air. The

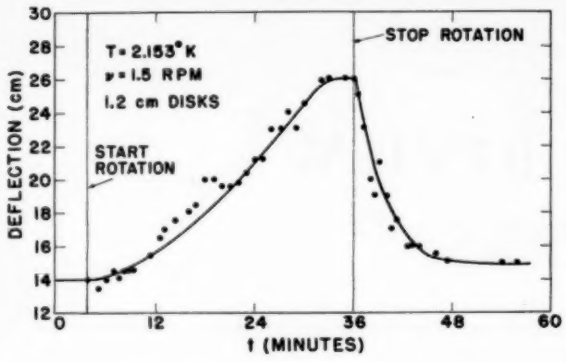

FIG. 1. Development of drag force on a disk in rotating He II. Rotation is begun at 4 minutes and stopped at 36 minutes.

calibrations were self-consistent to within about ±20%.

Three types of measurement were made with these detectors:

(1) For both systems the buildup of the drag forces with time after rotation was begun followed the same type of curve and had the same time scale as was found in the Rayleigh disk experiments.[1] That is, when rotation was started from rest a time delay was observed before any drag was seen, and the equilibrium drag was attained only after about $\frac{1}{2}$ hr. When rotation was stopped, the drag force immediately decreased, and the zero position was regained in a time much shorter than the buildup time. A typical drag versus time curve is shown in Fig. 1, for system I at a temperature of 2.153°K and 1.5 rpm. Rotation was begun at $t = 4$ minutes and stopped at $t = 36$ minutes. Thus in this experiment as well as in the Rayleigh disk experiments, there is evidence for a velocity front propagating from the walls upon initiation of rotation, and there is rigidity associated with the liquid upon cessation of rotation.

(2) The temperature dependence of the equilibrium drag force was studied in both systems at fixed rotational velocities. The results for system I are shown in Fig. 2 for a speed of 4.8 rpm. The drag force is seen to be almost independent of temperature from 1.3°K to the lambda temperature, T_λ, with a slight minimum near 1.9°K. The drag appears to be continuous across the lambda transition. However, above T_λ fluctuations in the detector became quite large, so that it was very difficult to take measurements and the points are subject to large error. The constancy of the drag force with temperature is in striking contrast with the torque measurements obtained with the Rayleigh disk.[1] The temperature variation of drag obtained with system II at fixed rotational velocities is similar to that for system I.

(3) At fixed temperatures below T_λ the drag force was studied as a function of the velocity (v) of rotation. For system I the drag force was found to be quadratic in velocity at all temperatures not too near T_λ. This is the velocity dependence expected for a disk immersed in a classical fluid at Reynolds numbers $\mathcal{R}$ greater than about 50.[2] In the present experiments, $\mathcal{R}$ ($=\rho v d/\eta_n$) always exceeds 100 so that classical drag may be expected. The dimensionless drag coefficient C_D (defined as the ratio of the observed drag force to $\frac{1}{2}\rho v^2$ times the area of the disk) ob-

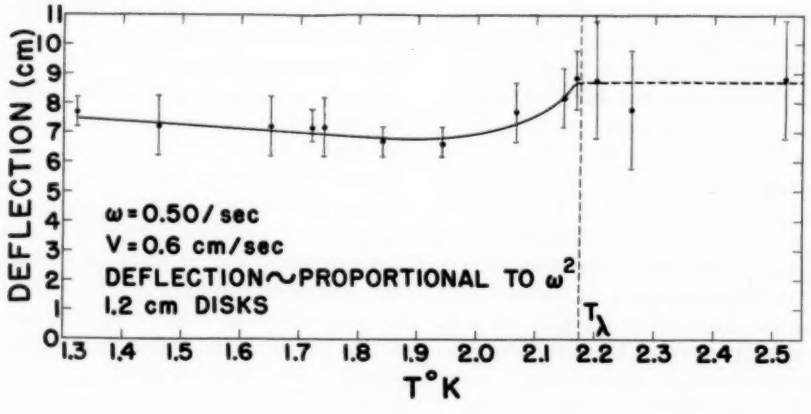

FIG. 2. Temperature dependence of the drag force on a disk in rotating helium.

tained from the data of Fig. 2 is about 0.25 at all temperatures. This drag coefficient is approximately equal to that obtained in the sphere drag measurements of Dowley, Firth, and Hollis Hallett,[3] an agreement which is somewhat surprising since the classical drag coefficient in this range of Reynolds numbers is 0.47 for spheres, while it is 1.17 for disks.[2] The behavior in the smaller system II was much different from system I. Except close to T_λ the drag force at fixed temperature varied as v^n with $1 \leq n < 1.3$. Figure 3 presents some representative drag versus rotational velocity measurements for systems I and II. At temperatures within 0.1°K of T_λ the behavior of both systems becomes more complicated. The exponent n becomes a function of velocity, but always approaches two at high velocities. The high-velocity drag coefficient is always about 0.25.

The significance of the linearity of the drag force with velocity in system II is not yet clear, and may well be an instrumental effect. This behavior and the behavior close to T_λ are still under study. However, because of the present lack of explanation for the Rayleigh disk results, we venture the following suggestion which offers a consistent method for interrelating those results with the linear drag found in the present experiment.

In classical fluids drag forces linear in velocity occur only for flow at low Reynolds numbers. The linearity of the system II measurements and the instantaneous decrease in the drag force upon cessation of rotation suggest that there is rigidity associated with rotating He II. This rigidity could arise from the vortex lines which must exist in rotating He II, and which probably exert drag forces upon bodies placed in rotating He II. Since the vortex lines are excitations of ground-state superfluid, they must be associated with the normal fluid, and would be seen in a drag experiment as an excess normal fluid viscosity. The Reynolds number describing the normal fluid flow would then be quite small, so that Stokes' drag linear in velocity could occur with attendant flow separation. Since the vortex line density is independent of temperature, the drag force is also. The line density is proportional to the rotational velocity, but the excess viscosity is not necessarily proportional to the line density. Such an excess normal fluid viscosity should influence the Rayleigh disk experiment. The equation for the torque on a Rayleigh disk is derived under the assumption of high Reynolds number flow with no flow separation. In rotating He II the total torque on a disk

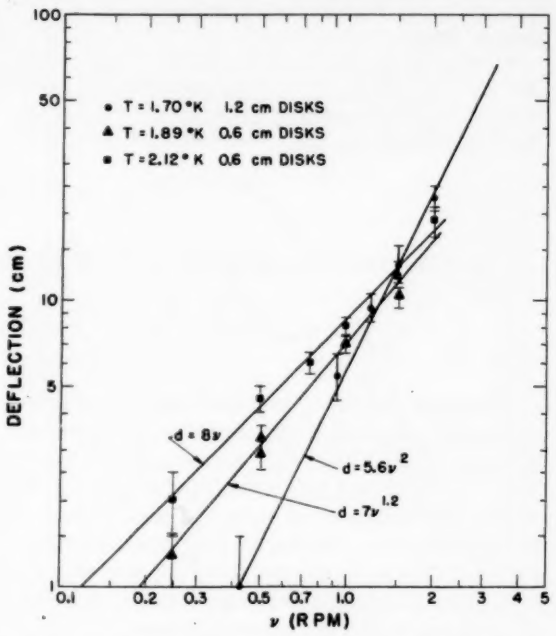

FIG. 3. Variation of the drag force on disks in He II with rotational velocity. Two distinct types of behavior are found.

with this assumption should be proportional to $\rho_s v_s^2 + \rho_n v_n^2$, and presumably $v_n = v_s$ since rotating He II is known to possess classical angular momentum.[4] If flow separation of the normal fluid occurs, the second term vanishes, and the total torque is proportional to $\rho_s v_s^2$, in agreement with Pellam's observations.

Vinen[5] has argued that vortex line turbulence may arise from heat currents in He II. If the above speculations are valid, it should be possible to increase the excess viscosity by heat currents. Preliminary experiments tend to support this idea, but large fluctuations of the detector due to unstable flow prevent definite conclusions at this time.

The author would like to thank Professor J. R. Pellam and Professor J. G. Dash for valuable discussions, and Mr. Donald Clinton and Mr. Earl McGowan for the construction of the apparatus, and for continuing advice on its design.

---

†Work performed under the auspices of the U. S. Atomic Energy Commission.

[1]J. R. Pellam, Phys. Rev. Letters 5, 189 (1960).
[2]S. F. Hoerner, Fluid Dynamic Drag (published by

the author, 148 Bustead Drive, Midland Park, New Jersey, 1958).

[3]W. W. Dowley, D. R. Firth, and A. C. Hollis Hallett, Proceedings of the Fifth International Conference on Low-Temperature Physics and Chemistry, Madison, Wisconsin, 1957, edited by J. R. Dillinger (University of Wisconsin Press, Madison, Wisconsin, 1958), p. 19.

[4]J. D. Reppy, D. Depatie, and C. T. Lane, Phys. Rev. Letters 5, 541 (1960).

[5]W. F. Vinen, Proc. Roy. Soc. (London) A242, 493 (1957).

EVIDENCE FOR SPIN-ORBIT SPLITTING IN THE BAND STRUCTURE OF ZINC AND CADMIUM*

A. S. Joseph, W. L. Gordon, J. R. Reitz, and T. G. Eck
Department of Physics, Case Institute of Technology, Cleveland, Ohio
(Received October 9, 1961)

Cohen and Falicov[1] have discussed the effect of spin-orbit coupling on the topology of the Fermi surfaces of the hexagonal close-packed metals. They conclude that spin-orbit splitting lifts the degeneracy between the first and second bands at the corners of the Brillouin zone and separates the small pockets of holes (arm caps) in the first band from the region of holes (arms) in the second. This gives rise to a closed-hole surface (cap surface) in the first band and a second-band surface that is infinitely extended along the hexagonal axis [Fig. 2(b) of reference 1] due to the intersections of arms. Both of these surfaces have extremal cross sections at the hexagonal face of the zone which one would expect to be observable in de Haas–van Alphen, cyclotron resonance, and ultrasonic attenuation experiments.

During the course of detailed de Haas–van Alphen studies of zinc and cadmium, we have observed oscillations in the magnetic susceptibility whose periods correspond to estimated values for the aforementioned extremal cross sections and which we have been unable to account for with Fermi surface models that neglect spin-orbit coupling. The de Haas–van Alphen periods were obtained by a torsion method in magnetic fields up to 23 kilogauss, using a null deflection technique and automatic recording. The angular dependences of the periods essential to this discussion are shown in Fig. 1. θ is the angle between the magnetic field direction and the hexagonal axis.

In Cd, for small θ the values of the Δ and x periods can be determined to within approximately 2% because all of the oscillations present are of comparable amplitude. As θ is increased the amplitude of the main arm oscillation increases rapidly, while effects due to arms in the other symmetry directions [periods indicated by dashed lines in Fig. 1(b)] are hardly observable. The amplitudes of the x and Δ oscillations drop rapidly, with Δ undetectable at $\theta \cong 1°$ and x at $\theta \cong 10°$.

In Zn, analysis is more difficult because x and Δ occur only as a weak modulation on a strong carrier—the arm periods. It was possible to obtain an unambiguous value for the Δ points out to a θ of 6°. However, there is no way of distinguishing from our data whether x lies below the arm period as shown in Fig. 1(a) or an equivalent distance above. The lower value was selected to be consistent with the relative sizes of the spin-orbit splitting in Zn and Cd (reference 1) and with the effect of this splitting on the difference in cross section of arm junction and cap surface as explained below. For θ greater than 7°, beating among the three arm periods makes detection of the Δ oscillation difficult due to its decreasing amplitude and to the presence of a comparable arm period. Therefore, the angular extent of the Δ period is not sharply determined. Near $\theta = 15°$, where the Δ period might beat distinctly with the arm periods, a careful search yielded no sign of its presence up to 23 kilogauss nor did any unexplained periods appear at larger θ.

The arm data in Zn agree with the few periods observed by Verkin and Dmitrenko,[2] while those in Cd fit very well with the work of Berlincourt,[3] but no mention of the x and Δ periods appears in either paper. We feel that the identification of Δ's as cap surface periods and x's as arm junction periods is correct because the other periods observed in Zn and Cd agree with the general form of portions of the Fermi surface predicted by the single orthogonalized plane wave construction,[4] and because this construction requires arm junctions and cap surfaces in the single zone scheme.

The presence of the spin-orbit energy gap decreases the cross section of the cap surface and increases that of the arm junction from the common value that these cross sections would have in

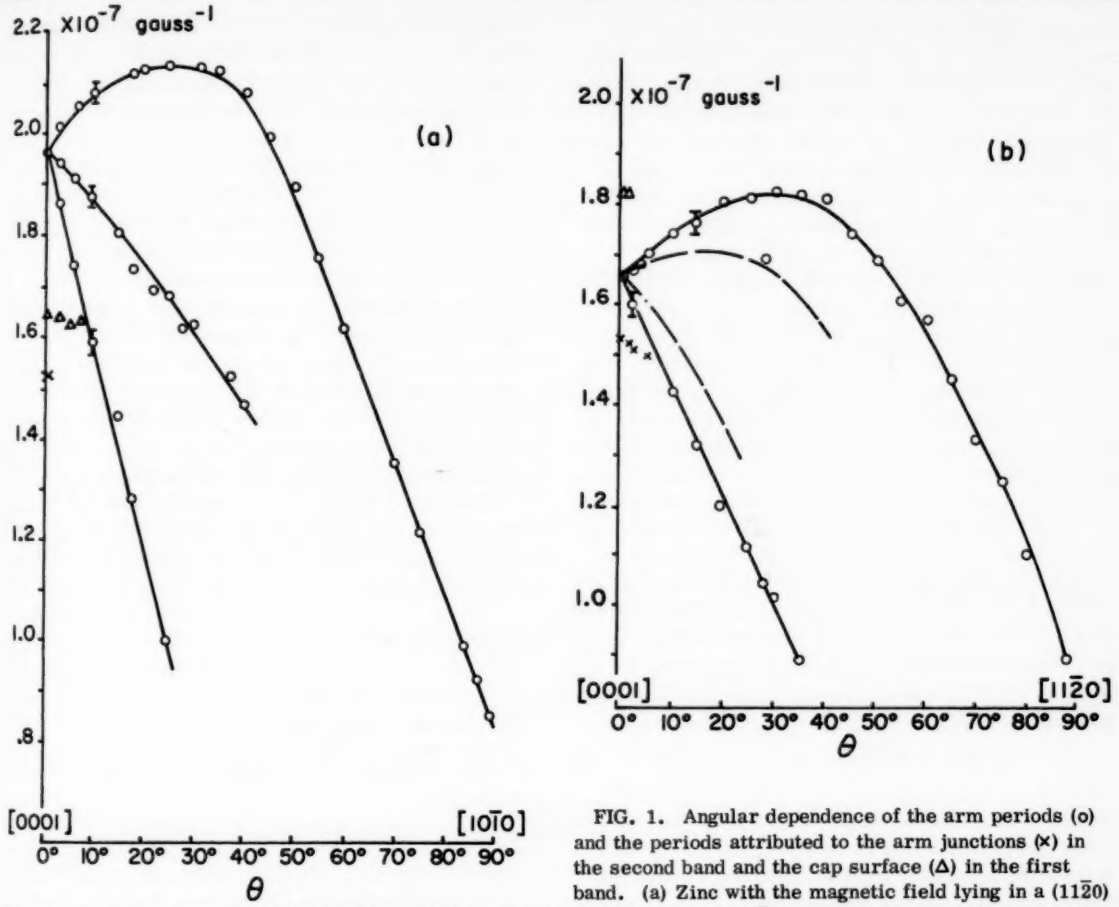

FIG. 1. Angular dependence of the arm periods (o) and the periods attributed to the arm junctions (×) in the second band and the cap surface (Δ) in the first band. (a) Zinc with the magnetic field lying in a (11$\bar{2}$0) plane (in reciprocal space). (b) Cadmium with the magnetic field lying in a (10$\bar{1}$0) plane (in reciprocal space). The dashed lines are drawn for the other arm periods expected using cross sections described by the full line.

the limit of a vanishing gap. If we use the nearly free electron approximation to estimate the influence of the size of the energy gap on the difference between cap surface and arm junction at the Brillouin zone face, the periods of Fig. 1 for magnetic field along the hexagonal axis yield a ratio of the spin-orbit energy gap in Cd to that in Zn of 2.2. This value is in reasonably good agreement with the estimate of 3 given in reference 1. The alternative possible assignment for the x period in Zn, discussed above, leads to an energy gap in Zn greater than that in Cd, an unlikely situation.

Our observation of periods due to the cap surface and arm junctions in Zn in magnetic fields as high as 23 kilogauss seems at first glance surprising in view of the possibility, first pointed out by Cohen and Falicov,[5] of "magnetic breakdown" of the spin-orbit energy gap. Blount[6] has shown that the relevant parameter determining breakdown is $\hbar\omega_c E_F/E_g^2$; i.e., when this quantity is much greater than one, the semiclassical electron orbits are determined by ignoring the energy gap in question. (Here ω_c is the cyclotron frequency, E_g is the energy gap, and E_F is the Fermi energy.) Using Cohen and Falicov's value for E_g in Zn,[1] we obtain for a field of 23 kilogauss a value for the above parameter that is of the order of one. Thus one would expect behavior characteristic of a transition region with additional scattering processes which would seriously decrease the amplitude of de Haas–van Alphen oscillations.

However, the criterion for breakdown should depend upon the inclination of the semiclassical orbit relative to the Brillouin zone plane under consideration. Intuitively, it would seem that if the electron's orbit cuts the Brillouin zone plane at a steep angle, then the probability for "jumping

the gap" ought to be higher than if the electron moves parallel to the zone plane. This result is borne out by detailed calculations; in fact, when the electron moves parallel to the zone plane, magnetic breakdown is completely inhibited. Thus, the spin-orbit energy gap across the hexagonal zone face in such metals should be seen, even at high fields, when the magnetic field is directed along the hexagonal axis of the crystal.

We have calculated the transition probability for scattering out of a semiclassical orbit as a result of the perturbation: $V = V_0 \cos(\vec{K}, \vec{r})$. According to nearly free electron theory, $E_g = 2V_0$. The method used is an alternative one to Blount's and is one suggested by Cohen.[7] We start with the transition probability per unit time due to scattering:

$$w = (2\pi/\hbar)\langle \textstyle\sum_{k'} |V_{kk'}|^2 \delta(E_{k'} - E_k) \rangle_k, \qquad (1)$$

where $\langle\ \rangle_k$ indicates an average over the orbit out of which the electron is being scattered. When the plane of the electron's orbit makes a small dihedral angle θ with the Brillouin zone plane, we obtain for the transition probability per cyclotron period:

$$w/\omega_c = E_g^2/32\hbar\omega_c \theta E_F \sin^2\phi, \qquad (2)$$

where ϕ is the polar angle of the electron's orbit (measured with respect to the magnetic field). When the orbit cuts the Brillouin zone plane at right angles, the calculation of w/ω_c may also be effected easily; the result for this case differs from (2) primarily through the deletion of the factor θ. By a WKB argument Blount[6] has shown that when $w/\omega_c \gg 1$, the probability for electron tunneling is $\exp(-\pi w/8\omega_c)$. Combining Eq. (2) with Blount's exponential factor and the E_g of reference 1 suggests that the effects of spin-orbit coupling should be observable within an angular range of about 6° from the hexagonal axis in zinc.

One would expect the arm junction period to exist over only a limited angular region due to the disappearance of an extremal cross section for this region of the Fermi surface, but the cap surface period should be present (barring magnetic breakdown) over the entire range of θ. We have observed the cap surface period for θ as large as 6° in Zn and 1° in Cd, and the arm junction period for θ as large as 1° in Zn and 10° in Cd. It is obvious from this that our data to date can cast little light on the question of the quantitative correctness of the present theory of magnetic breakdown.

We have been unable so far to observe cap surface and arm junction periods in magnesium.

We wish to thank J. W. Rutter and B. W. Roberts of the General Electric Research Laboratory at Schenectady for generously supplying the cadmium single crystal used in this work.

---

*This work has been supported in part by the Air Force Office of Scientific Research and in part by the U. S. Atomic Energy Commission.

[1]M. H. Cohen and L. Falicov, Phys. Rev. Letters 5, 544 (1960).

[2]B. I. Verkin and I. M. Dmitrenko, Izvest. Akad. Nauk S.S.S.R., Ser. Fiz. 19, 409 (1955) [translation: Bull. Acad. Sci. U.S.S.R., Phys. Ser. 19, 365 (1955)].

[3]T. G. Berlincourt, Phys. Rev. 94, 1172 (1954).

[4]W. A. Harrison, Phys. Rev. 118, 1190 (1960).

[5]M. H. Cohen and L. Falicov, Bull. Am. Phys. Soc. 6, 145 (1961); Phys. Rev. Letters 7, 231 (1961).

[6]E. I. Blount (to be published). We are indebted to Professor M. H. Cohen for informing us of Blount's results.

[7]M. H. Cohen (private communication).

REMARK CONCERNING QUANTIZED MAGNETIC FLUX IN SUPERCONDUCTORS

W. Brenig
Max-Planck-Institut für Physik und Astrophysik and Institut für Theoretische Physik, T. H. München, Germany
(Received August 7, 1961)

In a recent experiment,[1] the magnetic flux trapped within a doubly connected superconductor has been measured by cooling a thin ring embracing an external flux below the transition temperature. The experimental result is plotted in Fig. 1, which gives the total flux ϕ through the ring (which can never be changed in the superconducting state) as a function of the external flux ϕ_e. The quantity E also plotted in Fig. 1 will be discussed later on.

The unit $\phi_0 = hc/e$ of Fig. 1 is the unit of quantization briefly mentioned by London[2] and by Onsager[3] which stimulated the experiment. In order to find an indication for the quantization in units of $\phi_0/2$, let us first discuss the argument of London. After this we will give a simple argument that the experiment gives an indication of the existence of bound pairs in the superconductor.

If $\psi_0(\vec{r}_1 \cdots \vec{r}_N)$ is the wave function of the ground state of the superconductor, the wave function

$$\psi = \exp[i\textstyle\sum S(\vec{r}_i)/\hbar]\psi_0 \qquad (1)$$

corresponds to a superfluid flow with a velocity field $\vec{v}(\vec{r})$ given by

$$\vec{p}(\vec{r}) = \operatorname{grad} S(\vec{r}) = m\vec{v}(\vec{r}) + (e/c)\vec{A}(\vec{r}), \qquad (2)$$

thus obeying London's equation,

$$\operatorname{curl}[m\vec{v} + (e/c)\vec{A}] = 0. \qquad (3)$$

For a closed curve C located entirely within the superconductor and not embracing any hole, the integral

$$\oint_C \vec{p}\cdot d\vec{s} = \oint_C [m\vec{v} + (e/c)\vec{A}]\cdot d\vec{s} = (e/c)\phi \qquad (4)$$

therefore must be zero. This, however, need not be the case if C embraces a hole. As a consequence of (3) the integral then has the same value for all curves around the hole. If the ring is thick enough, the curve can be placed in its interior so that the current density $\sim\vec{v}(\vec{r})$ can be neglected. In this case one has $\phi = \int H df$.

The quantization of the flux ϕ then is supposed to follow from the fact that the wave function is single valued. London states, without proof, that this requires $\oint \vec{p}\cdot d\vec{s} = nh$. This sounds plausible since ψ_0 is single valued so that $\exp[i\sum S(\vec{r}_i)/\hbar]$ also has to be single valued in order to guarantee the same for ψ.

We now want to show that this is not necessary if ψ_0 contains strong correlations of the kind proposed by Bardeen, Cooper, and Schrieffer.[4]

According to BCS the ground-state wave function can be written as

$$\psi_0 = A\prod_{i<j} w(\vec{r}_i - \vec{r}_j), \qquad (5)$$

where A indicates the antisymmetrization procedure and $w(\vec{r})$ is the Fourier transform of $v_k/u_k = w_k$ (u_k and v_k being defined as in BCS).

Let us now introduce cylinder coordinates with the axis along the axis of the ring. If we do not indicate the r and z dependence explicitly, (5) reduces to

$$\psi_0 = A\prod w(\varphi_i - \varphi_j). \qquad (6)$$

As a first approximation one may expect $w(\varphi_2 - \varphi_1)$ to be similar to the wave function in an infinitely extended homogeneous superconductor, i.e., only different from zero in the neighborhood of $\varphi_1 = \varphi_2$, which would be single valued in $(\varphi_1 + \varphi_2)/2$ but not in φ_1 and φ_2 individually. The latter would require

$$w(\varphi) = w(\varphi + 2\pi). \qquad (7)$$

This condition, however, can be fulfilled in replacing w by

$$w_g = \textstyle\sum_\nu w(\varphi + 2\pi\nu). \qquad (8)$$

One also expects excited states corresponding

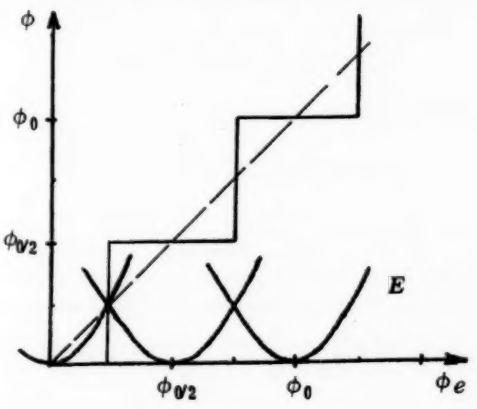

FIG. 1. The experimental values of ϕ (step-like curve, schematically) and the kinetic energy E of the superconductor as function of ϕ_e.

to pairs running around the axis with a total angular momentum n of the type

$$e^{in(\varphi_1+\varphi_2)/2} w_g(\varphi_2-\varphi_1). \quad (9)$$

Here n has to be an integer in order to make (9) single valued in $(\varphi_1+\varphi_2)/2$. The single valuedness in φ_1 and φ_2 individually can be saved if w_g is replaced by

$$w_u=\sum_\nu w(\varphi+2\pi\nu)(-1)^\nu, \quad (10)$$

if n is odd.

The wave functions (9) and (10) are not exact eigensolutions of the Schrödinger equation, but they are good approximations deviating from the solutions of the homogeneous medium in only a very small part of the configuration space $0 \leq \varphi_1, \varphi_2 < 2\pi$ if the extension of the pairs is small compared to the dimensions of the ring. The wave functions of the whole system are given by

$$e^{in\sum_i \varphi_i/2} A\prod w_g(\varphi_i-\varphi_j) \text{ for } n \text{ even},$$

$$e^{in\sum_i \varphi_i/2} A\prod w_u(\varphi_i-\varphi_j) \text{ for } n \text{ odd}. \quad (11)$$

We do not consider excitations corresponding to the breakup of pairs and the acceleration of a pair relative to the rest of the pairs since these are only excited by fields above the critical field. The application of (4) then gives the required half-integral values of $e\phi/hc$.

The discussions above only give the wave functions which are compatible with the requirement of single valuedness but do not tell us which of them actually is obtained for a given external flux. For this purpose let us consider the energy of the electrons as a function of the external flux ϕ_e. Since there is no first order change of the wave function of a superconductor in an external field, the energy of the excited states above the ground state is just the kinetic energy of the superfluid flow which can be estimated by assuming $v(r)$ to be constant inside the penetration depth and zero outside. This gives as the excitation energy per particle

$$E/N=\tfrac{1}{2}mv^2(\lambda/\Delta r), \quad (12)$$

where Δr is the thickness of the ring and λ the penetration depth.

The velocity v then can be calculated from Maxwell's equation: $|\mathrm{curl}\,\vec{H}| = 4\pi n_s ev/c$ (n_s is the number of superconducting electrons). If one replaces $\pi r^2 H$ by the flux $(\phi-\phi_e)$ produced by the superconducting electrons, one obtains finally

$$n_s ev=(\phi-\phi_e)c/4\pi r^2\lambda; \quad E=\mathrm{const}(\phi-\phi_e)^2. \quad (13)$$

The result is plotted in Fig. 1 for different values of the total flux ϕ.

Whereas in the superconducting state the transitions between different parabolas, even if energetically possible, are forbidden because of $d\phi/dt=0$, one expects that the state obtained by cooling the ring down from the normal state with an external flux will be the state of lowest possible energy, i.e., that state which can be obtained by the smallest possible acceleration of the electrons. This would explain completely the experimental result of Fig. 1, in particular the fact that the first flux quantum is trapped already if the external flux has only reached the value of $\phi_0/4$.

The model considered above is of course very poor. We have only treated the case of zero temperature and we have left out all the complicated events which happen during the transition from the normal to the superconducting state. Nevertheless we hope that the indications are strong enough to believe that the experiment of Doll and Näbauer is a (macroscopic) consequence of angular momentum quantization (similar to the quantized vortex lines in He II) and is directly related to the existence of bound pairs of electrons in the superconductor.

Note added in proof. Meanwhile there has appeared a Letter by Onsager[5] explaining the occurrence of odd multiples of $hc/2e$ in essentially the same way as above. We can use our wave function to exhibit the equivalence of this idea to the pairing condition as used by Byers and Yang.[6] For this purpose one only has to notice that introducing

$$w_\nu=\frac{1}{2\pi}\int_{-\infty}^{\infty} w(\varphi)e^{-i\nu\varphi}d\varphi,$$

w_g and w_u can be written as

$$w_g=\sum_\nu w_\nu e^{i\nu\varphi},$$

$$w_u=e^{-i\varphi/2}\sum_\nu w_{\nu+1/2}e^{i\nu\varphi}. \quad (14)$$

The wave functions (11) then can easily be transformed to the usual notation in second quantization:

$$\prod(u_\nu+v_\nu a_{\uparrow\nu+m}{}^* a_{\downarrow-\nu+m}{}^*)|0\rangle; \quad (n \text{ even})$$

$$\prod(u_{\nu+1/2}+v_{\nu+1/2}a_{\uparrow\nu+m+1}{}^* a_{\downarrow-\nu+m}{}^*)|0\rangle; \quad (n \text{ odd}) \quad (15)$$

with $n=2m$ ($n=2m+1$) for even (odd) values of n.

Inside a thick ring the kinetic angular momenta are given by $\hbar(\nu - e\phi/hc)$ if $\hbar\nu$ is the canonical angular momentum. Therefore with $\phi = hcm/e$ $[\phi = hc(m+\frac{1}{2})/e]$ the pairing with zero current occurs for $(\nu, -\nu)$ $[\nu+\frac{1}{2}, -\nu-\frac{1}{2})]$ in the case of even (odd) n. The description in terms of wave functions (11) or (15) has the advantage of not only showing the equivalence of two apparently different pictures but also of being valid in the case of thin rings where the current does not vanish as assumed by Byers and Yang.

We wish to thank H. P. Duerr, W. Heisenberg, H. Koppe, M. Näbauer, A. de-Shalit, and V. F. Weisskopf for stimulating discussions.

[1]R. Doll and M. Näbauer, Phys. Rev. Letters 7, 51 (1961), and B. S. Deaver and W. M. Fairbank, Phys. Rev. Letters 7, 43 (1961).

[2]F. London, Superfluids (John Wiley & Sons, New York, 1950), p. 152.

[3]L. Onsager, Proceedings of the International Conference of Theoretical Physics, Kyoto and Tokyo, 1953 (Science Council of Japan, Tokyo, 1954), pp. 935-936.

[4]J. Bardeen, L. N. Cooper, and J. R. Schrieffer, Phys. Rev. 108, 1175 (1957), quoted as BCS.

[5]L. Onsager, Phys. Rev. Letters 7, 50 (1961).

[6]N. Byers and C. N. Yang, Phys. Rev. Letters 7, 46 (1961).

OSCILLATORY GALVANOMAGNETIC EFFECT IN METALLIC SODIUM*

R. Bowers, C. Legendy, and F. Rose

Laboratory of Atomic and Solid-State Physics and Department of Physics, Cornell University, Ithaca, New York

(Received October 5, 1961)

We wish to report the observation at 4°K of a novel galvanomagnetic effect in sodium of very high conductivity ($\rho_{300°K}/\rho_{4°K} \approx 7500$; $\omega_c\tau \approx 40$ in 10 000 gauss). In this effect, the Lorentz force produces an electrical oscillation of low frequency (ranging from 5 to 35 cycles/sec in our experiment). Our results provide direct evidence of a particular macroscopic electron gas excitation described by Aigrain[1] and given by him the name "helicon" excitation. There is also a connection between our observation and certain effects observed in bismuth at microwave frequencies.[2]

The experimental arrangement (Fig. 1) is based on a configuration for measuring resistivity due to Bean, DeBlois, and Nesbitt.[3] A cylindrical specimen of sodium (height 30 mm and diameter 4 mm) is placed inside primary and secondary coils. On closing or opening the primary circuit, eddy currents are induced in the specimen which can be detected by the secondary coil. From the time constant of the observed voltage in the secondary, one can estimate the resistivity of the specimen. For a sufficiently long time after the primary pulse, the decay is a simple exponential. Our experiment differs from that in reference 3 in that a constant magnetic field (H_0) is applied perpendicular to the axis of the specimen and coils. The constant field H_0 is much larger than the time-dependent magnetic field ($h \approx$ few hundred gauss) produced by the primary coil. The voltage of the secondary coil is observed on closing or opening the primary circuit. Figure 2 shows oscilloscope traces of the secondary voltage as a function of time for various values of the bias field H_0, using sodium for which $\rho_{300°K}/\rho_{4°K} \approx 7500$ (mean free path at 4°K $\approx \frac{1}{4}$ mm). In zero magnetic field the normal eddy current decay is observed. The other three traces show the effect of applying H_0. One sees damped oscillations whose frequency is proportional to magnetic field. The frequency at 10 000 gauss is 32 cycles/sec.

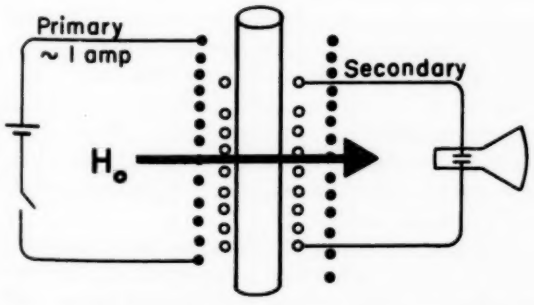

FIG. 1. Schematic diagram of experiment. Primary coil ≈300 turns of No. 28 copper wire; secondary coil ≈1200 turns of No. 43 copper wire. Specimen and coils immersed in liquid helium at 4.2°K.

We believe the oscillations to originate as follows. The abrupt change in the primary field (h) excites stable modes of the electron gas in which the electric vector is circularly polarized about the large magnetic field.[1] The oscillation observed is the component of this circular wave resolved in

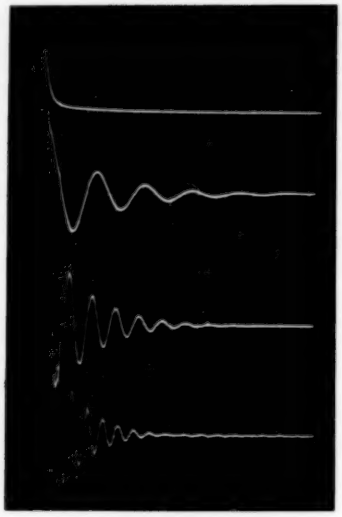

FIG. 2. Voltage in secondary coil as a function of time on opening primary circuit for different values of H_0. Starting from the top, the four curves correspond to $H_0 = 0$, 3600, 7200, and 10 800 gauss, respectively. Ordinate is 5 millivolts per large division; abscissa is 50 milliseconds per large division. Specimen properties: $\rho_{300°K}/\rho_{4°K} \approx 7500$; $\omega_c\tau \approx 40$ in 10 000 gauss.

the direction of the axis of the secondary coil. A precise theory of this effect requires the solution of the field equations with the complicated boundary conditions used in our experiment. However, a useful physical picture of the origin of the circularly polarized waves can be derived from the following simplified theory for the infinite solid of very high conductivity.

In a strong magnetic field ($\omega_c\tau \gg 1$), the current vector and the electric field vector are nearly perpendicular, as the component of the electric field along the current direction becomes very small compared to the transverse (Hall) field. We therefore write[4]

$$\vec{E} + \mu_0 \vec{v}_D \times \vec{H} = 0,$$

$$\vec{I} = ne\vec{v}_D, \qquad (1)$$

using rationalized mks units and conventional notation. We use Eq. (1) for fields and currents varying in space and time, assuming that the mean free path and the relaxation times are short compared to the corresponding periods in the solutions. From Eq. (1) and Maxwell's equations (neglecting displacement current) it follows that

$$\partial\vec{E}/\partial t = (1/ne)[\nabla \times (\nabla \times \vec{E})] \times \vec{H}_0, \qquad (2)$$

assuming that $\vec{H} = \vec{H}_0 + \vec{h}(\vec{r}, t)$, $|\vec{H}_0| \gg |\vec{h}|$, and $\vec{H}_0$ is along the z axis. We solve by substituting $\vec{E} = \vec{E}_0 \exp[i(\omega\tau - \vec{k}\cdot\vec{r})]$. Equation (2) reduces to a set of three linear homogeneous equations for the components of E_0. The secular equation yields two nonzero frequencies for any given wave vector $\vec{k}$:

$$\omega = \pm k k_z H_0/ne. \qquad (3)$$

The corresponding solutions, omitting a common multiplicative constant, are:

$$\vec{E}_0 = (k_x^2 + k_z^2, k_x k_y \pm i k k_z, 0),$$

$$\vec{h}_0 = (k_z/\omega\mu_0)(-k_x k_y \mp i k k_z, k_x^2 + k_z^2, -k_y k_z \pm i k k_x),$$

$$\vec{I}_0 = \mp k \vec{h}_0.$$

For propagation along the z direction, these reduce to $k^2(1, \pm i, 0)$; $(k^3/\omega\mu_0)(\mp i, 1, 0)$; $\mp k\vec{h}_0$, respectively. All the above solutions describe circularly polarized plane waves, the two signs corresponding to right-hand and left-hand screw spatial configurations. The vectors rotate about the magnetic field lines always in the direction corresponding to the cyclotron rotation of the carriers. The $\vec{E}$ field in general has a component along the propagation direction; the $\vec{h}$ and $\vec{I}$ fields do not.

At 10 000 gauss the observed frequency was 32 cycles/sec; with these values Eq. (3) yields a half-wavelength of 3.4 mm for a wave that propagates along the field lines. This is comparable with the corresponding specimen dimension which is 4 mm. The observed linear dependence of the frequency on the magnetic field is also in agreement with Eq. (3).

We have not been able to find any other explanation for the observed oscillations. Mechanical oscillations of the coil in the magnetic field are expected to produce an oscillation whose frequency is determined by the mechanical spring constants and is independent of H_0; the amplitude of the resulting oscillations would depend on H_0 in a manner quite different from that shown in Fig. 2. Moreover, we have taken care to reduce mechanical effects to the minimum. The oscillations observed occur at frequencies which are too low by orders of magnitude to be associated with Landau levels.

The simple theory predicts that the frequency should be independent of conductivity in the high-conductivity limit. This was verified on investigating the oscillation in four sodium specimens whose residual resistance ratios were 7500, 4500, 3200, and 1200, respectively. It was found that oscillations were more damped as the conductivity

decreased but the frequency did not change appreciably. At a ratio of 1200, no oscillations were found because of excessive damping, indicating that the conductivity must be very high in order to see the oscillations. Sodium is very favorable in this respect since it has a very small magnetoresistance.

In a variation of the experiment described above, the oscillation was excited under resonant conditions. Helmholtz coils were mounted (outside the cryostat) so that their axis was perpendicular both to the large field H_0 and to the axis of the secondary coil. The latter orientation reduces direct mutual inductance coupling. In Fig. 3 is shown the response of the secondary to a sinusoidal excitation of the Helmholtz coils; the specimen was the same as that used for Fig. 2. The amplitude of excitation current was maintained constant and the frequency varied. A resonant response was obtained. From studies of different specimens, it was found that the Q for the resonance increases with increasing conductivity but the resonant frequency is nearly independent of the conductivity in the range investigated. As yet, no identifiable harmonics have been found. Although the dependence of the resonance on specimen size has not been investigated in detail, it is observed that the resonant frequency increases as the length along H_0 is decreased.

We expect to carry out experiments in which the geometrical arrangement is more amenable to detailed theoretical analysis than the present arrangement; this requires modification of our magnet-cryostat system. This work provides further evidence that one can study in a solid some of the macroscopic electron gas excitations more frequently investigated in gaseous plasmas.[2]

We are indebted to J. Krumhansl and M. T. Taylor for helpful discussions, and to S. Tallman and E. Johnson for contributions to the experiment. The high-purity sodium was prepared by C. E. Taylor of the Lawrence Radiation Laboratory, Livermore, California.

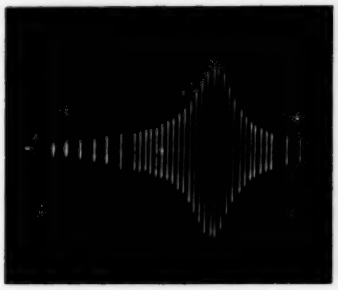

FIG. 3. Voltage in secondary as a function of frequency of exciting coil for fixed $H_0 = 10\,800$ gauss. Ordinate is 1 millivolt per large division; abscissa is 5 cycles/sec per large division. Specimen was the same as that used for Fig. 2.

---

*This work was supported by the U. S. Atomic Energy Commission and the Advanced Research Projects Agency.

[1]P. Aigrain, Proceedings of the International Conference on Semiconductor Physics, Prague, 1960 (Publishing House of the Czechoslovak Academy of Sciences, Prague, 1961), p. 224; P. Weiss and P. Nozières (unpublished).

[2]J. K. Galt, W. A. Yager, F. R. Merritt, and B. B. Cetlin, Phys. Rev. 114, 1396 (1959); S. J. Buchsbaum and J. K. Galt, Phys. Fluids (to be published).

[3]C. P. Bean, R. W. DeBlois, and L. B. Nesbitt, J. Appl. Phys. 30, 1976 (1959).

[4]R. G. Chambers, in The Fermi Surface, edited by W. A. Harrison and M. B. Webb (John Wiley & Sons, New York, 1960), p. 102.

CRITICAL POINTS AND FERROMAGNETISM

E. P. Wohlfarth and J. F. Cornwell*
Department of Mathematics, Imperial College, London, England
(Received October 16, 1961)

Ordinary and some singular critical points of $E(\vec{k})$ in the Brillouin zones of metals produce infinite discontinuities of $N'(E)$, the derivative with respect to energy E of the density of states $N(E)$.[1,2] As a result, $N(E)$ curves contain a number of sharp and narrow peaks, the structure being more pronounced for the more complicated metals. This is illustrated in Fig. 1, showing $N(E)$ for body-centered iron. The curve was calculated, as described by us previously,[3] by applying the Slater-Koster interpolation scheme[4] to the results of Wood,[5] who used the augmented plane wave method but did not, according to the present calculations,[3] cover a sufficient number of points in the zone to give a fully reliable $N(E)$ curve, nor did he investigate the critical points.

The $N(E)$ curve of reference 3 was obtained by finite difference methods and thus also did not exhibit the sharp peaks of the curve of Fig. 1; this was calculated by numerical differentiation. Further consideration of this curve has now become of interest, for the following reason: The peaky structure, here exemplified for iron but present for all metals,[6] seems to have a direct bearing on the occurrence of ferromagnetism, and may thus explain the recently discovered ferromagnetism in the Sc-In alloy system[7]; the properties of iron itself may also be discussed on this basis.[3]

It is thus suggested that on adding indium to scandium the Fermi energy passes through a very narrow peak in $N(E)$ corresponding effectively to the very narrow composition range 23.8% to 24.2% In over which ferromagnetic behavior was found to occur so sensitively. The low value of the Curie temperature T_C, observed to be about 6°K for these alloys, is then related to the low effective

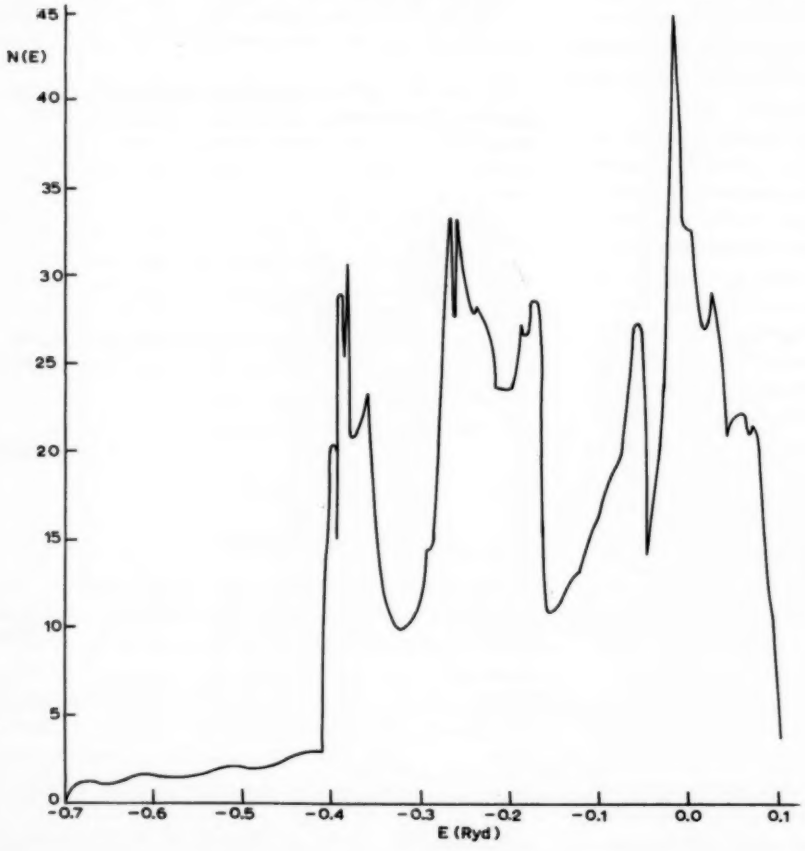

FIG. 1. Density-of-states curve for body-centered iron. $N(E)$, density of states per atom; E, energy in rydbergs.

degeneracy temperature proportional to the width of the peak. The susceptibility χ above T_c could only be calculated if the precise structure of the peak and the exchange energy were known. However, as exemplified in Fig. 7 of Elcock et al.,[8] and as frequently discussed for normal ferromagnetic metals and alloys,[9] the $1/\chi, T$ curves calculable on this basis frequently appear to be very closely linear over relatively wide ranges of temperature above T_c. The slopes of such linear curves then bear no relation whatever to the saturation magnetizations obtained from low-temperature measurements. For the Sc-In alloys there was indeed no such relation: The saturation magnetic moments per atom are given as 0.035 to 0.039 Bohr magneton while the values derived from the apparent Curie-Weiss constants ranged from 0.65 to 0.70 over the ferromagnetic composition range. This divergence shows that a localized model is not applicable here, while the discussion just given shows that the observations can be explained in terms of a band model including a peaky structure. Further evidence bearing on this interpretation would come from low-temperature specific heat measurements.

We wish to thank B. T. Matthias and A. M. Clogston for helpful discussions of their results.

---

*Present address: Department of Mathematics, Leeds University, Leeds, England.

[1]L. Van Hove, Phys. Rev. 89, 1189 (1953).

[2]J. C. Phillips, Phys. Rev. 104, 1263 (1956).

[3]J. F. Cornwell and E. P. Wohlfarth, Conference on Magnetism and Crystallography, Kyoto, September, 1961 [J. Phys. Soc. Japan (to be published)].

[4]J. C. Slater and G. F. Koster, Phys. Rev. 94, 1498 (1954).

[5]J. H. Wood, Quarterly Progress Report, Massachusetts Institute of Technology Solid State and Molecular Theory Group, January 15, 1961 (unpublished), p. 79.

[6]J. F. Cornwell, Proc. Roy. Soc. (London) A261, 551 (1961).

[7]B. T. Matthias, A. M. Clogston, H. J. Williams, E. Corenzwit, and R. C. Sherwood, Phys. Rev. Letters 7, 7 (1961).

[8]E. W. Elcock, P. Rhodes, and A. Teviotdale, Proc. Roy. Soc. (London) A221, 53 (1953).

[9]E. P. Wohlfarth, Proc. Roy. Soc. (London) A195, 434 (1949).

NUCLEAR SPIN STATES IN MOLECULAR CRYSTALS*

L. B. Borst, S. L. Borst, L. Koysooko,† H. Patel, and E. Stusnick
Department of Physics, New York University, University Heights, New York, New York
(Received August 21, 1961; revised manuscript received October 9, 1961)

Nuclear spin states are commonly identified in gases, but are not generally expected to exist in condensed phases. Whereas ortho and para forms are acknowledged for hydrogen both in liquid and solid,[1] restrictions in other cases imposed by neighboring molecules presumably prevent quantized rotation with a clear distinction between odd and even rotational quantum numbers with associated parallel and antiparallel nuclear spin alignment.

In the case of molecular hydrogen, the elastic neutron scattering cross section for the ortho state is large compared to the para state for both liquid and gas (30:1 in the case of the gas).[2] Neutron scattering measurements therefore permit the identification of ortho and para states.

The experiment consisted of measuring the attenuation of a neutron beam by the sample under investigation which was immersed in liquid helium. Temperatures below 4°K were achieved by evacuating the liquid helium and reducing the boiling point. The beam intensity as measured by a thin BF_3 counter was observed as a function of time with sudden changes in sample temperature, holding other experimental parameters constant. The neutron beam was derived from a reentrant hole in an aqueous moderator immersed in liquid helium. A velocity spectrum of the emergent beam was best fitted by a Maxwell distribution having a temperature of 40°K.

Solid acetylene (HCCH), a linear molecule, was cooled, first to 4°K and then to 2°K, and the total cross section was followed as a function of time (Fig. 1). The cross section changed from an initial value of 140 barns to 10 barns per molecule. The temperature was rapidly raised to 77°K, after which the cross section returned to its original value. The time for 50% conversion from the low-temperature form (mostly para) to high-temperature form (3 ortho-1 para) was about 10 minutes.

Heat capacity data for water were once interpreted in terms of ortho and para states.[3] The Pauling model[4] so completely explained the residual entropy that the alternate interpretation was

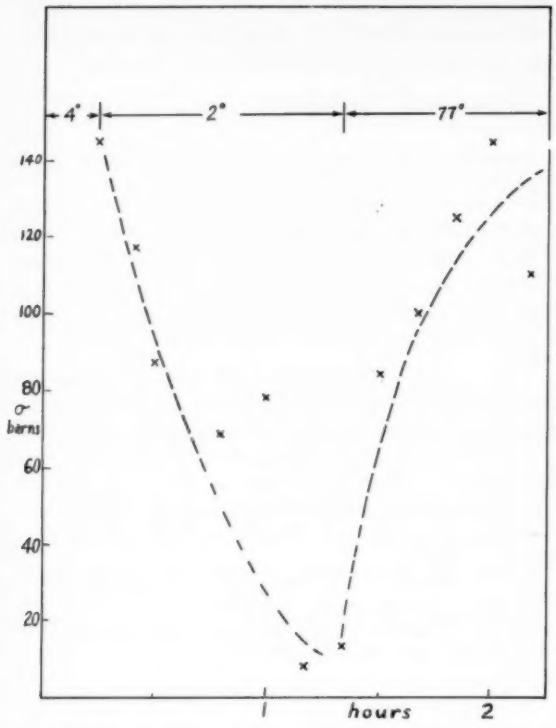

FIG. 1. Time-dependent cross section of acetylene.

forgotten. Comparison of the scattering cross section of molecular hydrogen with water for the high-temperature mixture (3 ortho-1 para) shows comparable cross sections and energy dependence. Even though hydrogen-bonded, water would seem to have ortho and para modifications.[5,6] Transmission experiments similar to those on acetylene confirm this prediction.

Water has been studied as a neutron moderator at cryogenic temperatures.[6,7] Allowed transitions between ortho and para states are possible by means of spin exchange scattering. This inelastic process constitutes an additional moderation mechanism.[5] A kilogram sample was cooled to 4°K. The neutron spectrum within the moderator, as measured by a foil activation technique, indicated the existence of a substantial fraction of the neutrons in a Maxwell distribution near the thermodynamic temperature.[6] A beam of neutrons was removed under geometric conditions which assured minimum perturbation of the velocity distribution function.

An absorption curve, using $1/v$ absorber and a thin $1/v$ detector, showed that 20% of the neutrons in the beam from a 4° moderator had an effective cross section in indium of 1500 barns. This soft component was not present at moderator temperatures of 77 or 300°K. These data are considered evidence that 20% of the neutrons reaching 300°K enter a thermal distribution near 4°K. All the foregoing experiments were conducted immediately after cooling the moderator and were conducted within a period of less than an hour.

A velocity spectrum did not, however, clearly delineate this low-temperature thermal distribution. Plotting the intensity per channel as a function of time disclosed an exponential decay with a half-life of about 100 minutes (Fig. 2). Under the experimental conditions of constant moderator temperature and careful monitoring, the intensity change could only be identified with a change in the scattering power of the moderator. A reduction in scattering power would increase the leakage of neutrons from the refrigerated moderator, thereby reducing the thermal source intensity. At the end of the refrigeration period the thermal neutron distribution returned to its original intensity. A change in intensity by a factor of ten was observed in the course of eight hours for neutrons between 500 and 1500 μsec/m reciprocal velocity. The channel covering 0-500 μsec/m shows a less pronounced time dependence because it includes fast and epithermal neutrons.

These changes in spectral intensity are considered evidence of substantial ortho to para transformation with associated loss of scattering power. After para transformation, the neutron flux is so low that it is not possible to distinguish a Maxwell distribution near the thermodynamic temperature from background effects. During the first part of the experiment, when ortho molecules are present, and earlier measurements showed evidence of a Maxwell distribution near the thermodynamic temperature, velocity selector statistics are inadequate again to demonstrate its existence.

Water is therefore an ineffective neutron moderator at 4°K. In the para state no levels exist near the ground state so that there is no effective mechanism for inelastic scattering and neutron moderation. While the ortho state has an appropriate transition for neutron energy loss, the lifetime of the ortho molecule for spontaneous transformation to para is short. If the temperature is such that a significant fraction of the molecules exist in the ortho state, then its neutron moderating properties should be good.

Nuclear spin states found in water and acetylene are expected in many molecular crystals, the rotational energy levels being shifted to higher tem-

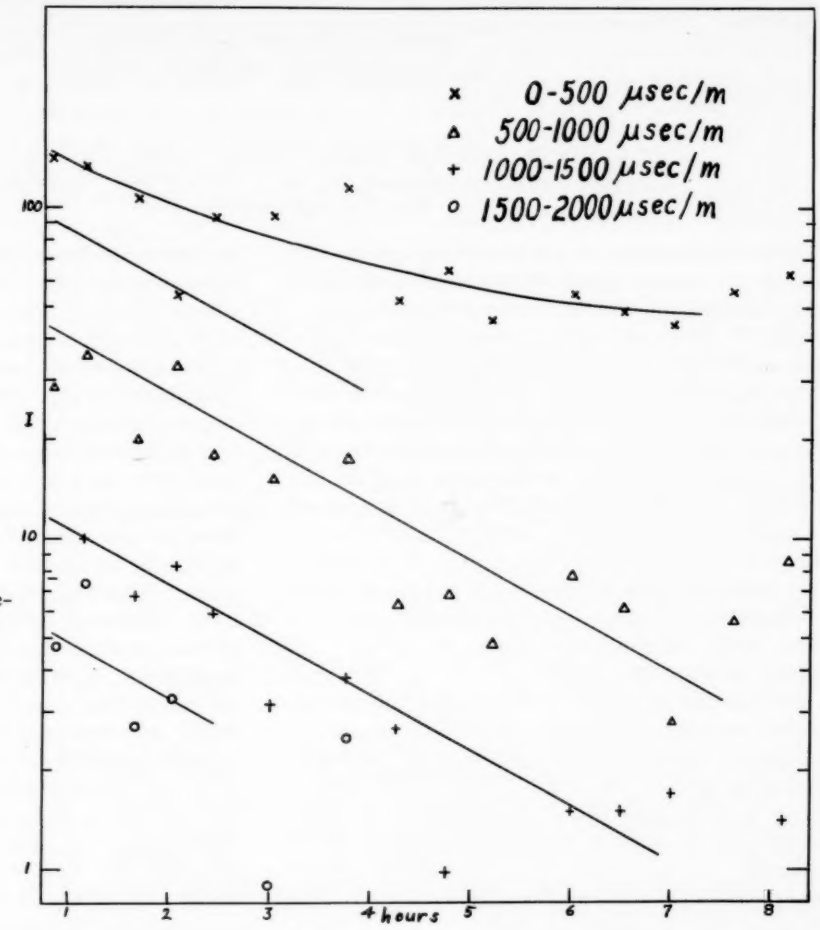

FIG. 2. Time-dependent spectral distribution from aqueous moderator at 4°K.

peratures by the crystal potential. Neutron scattering is an incisive tool at least in the case of dihydrogen molecules because of the large change in scattering power between ortho and para states. Crystal structure determinations using neutrons must now be reviewed in the light of these observations, particularly in the case of water.

*Research supported by John S. Barnes Corporation and the National Science Foundation.

†International Atomic Energy Authority Fellow from Thailand.

[1]A. Farkas, Orthohydrogen, Parahydrogen, and Heavy Hydrogen (Cambridge University Press, New York, 1935).

[2]R. B. Sutton et al., Phys. Rev. 72, 1147 (1947).

[3]W. F. Giauque and J. W. Stout, J. Am. Chem. Soc. 58, 1144 (1936); E. A. Long and J. D. Kemp, J. Am. Chem. Soc. 58, 1829 (1936).

[4]L. Pauling, J. Am. Chem. Soc. 57, 2680 (1935).

[5]L. B. Borst, Phys. Rev. Letters 4, 131 (1960).

[6]L. B. Borst, International Atomic Energy Agency Symposium, Vienna, October, 1960 (to be published), Paper No. IS/30.

[7]A. W. McReynolds and W. L. Whittemore, International Atomic Energy Agency Symposium, Vienna, October, 1960 (to be published), Paper No. IS/33.

NEW DETERMINATION OF THE K^+-DECAY BRANCHING RATIOS*

Byron P. Roe and Daniel Sinclair
University of Michigan, Ann Arbor, Michigan

and

John L. Brown, Donald A. Glaser,† John A. Kadyk, and George H. Trilling†
Lawrence Radiation Laboratory, University of California, Berkeley, California
(Received September 28, 1961)

Present knowledge of the branching ratios among the various decay modes of K^+ mesons has come exclusively from emulsion measurements.[1-3] The results of the most precise emulsion determinations are presented in the first three columns of Table I. Since some of the experimental values of the branching ratios are in disagreement by substantially more than the errors assigned, we have remeasured them using a different technique in order to obtain a new and independent set of values. The high efficiency for conversion of gamma rays from π^0 mesons into electron pairs and the ease of recognition of electrons in a xenon bubble chamber[4] have been used to separate the various K^+-decay modes in our experiment.

The results presented in this Letter are based on the analysis of a sample of 6300 K^+ mesons obtained from an exposure of the xenon chamber to a separated 700-Mev/c K^+ beam at the Bevatron. A moderator was used to reduce the beam momentum to about 400 Mev/c at the entry of the chamber, so that the K^+ mesons came to rest and decayed near the center of the chamber. The chamber has no magnetic field.

The scanning and measurement of the photographs led to the classification of the events into various categories. The requirements that characterize each of these categories are given below, followed in parentheses by a list of the K^+-decay modes that are the main constituents of the events classified therein: (a) events with more than one charged secondary (τ); (b) events with a single-charged secondary and three or four electron pairs (τ'); (c) events with two, one, or zero electron pairs and a charged secondary clearly identified as an electron by its large radiative energy loss or its production of a cascade shower (K_{e3}).

The remaining events were classified as follows: (d) events with a single-charged secondary and two electron pairs identified to be $K_{\pi 2}$ by the constraints imposed in the application of energy and momentum conservation to K^+ and π^0 decays ($K_{\pi 2}$); (e) events not in Category (d) which have a single-charged secondary and two electron pairs ($K_{\mu 3}, \tau'$); (f) events with a single-charged secondary and one electron pair ($K_{\pi 2}$, $K_{\mu 3}$); (g) events with a single-charged secondary and no electron pairs ($K_{\mu 2}$).

The μ secondary from a π^+ decay at rest has a range of only 1.3 mm and hence cannot always be reliably identified. Thus no separation was made

Table I. K^+ branching ratios, in percent.

Decay mode	Birge et al.[a]	Alexander et al.[b]	Taylor et al.[c]	Present expt.	ΔB for 2% change in γ scanning efficiency
$K_{\mu 2} \rightarrow \mu^+ + \nu$	58.5 ± 3.0	56.9 ± 2.6		64.2 ± 1.3	0.2
$K_{\pi 2} \rightarrow \pi^+ + \pi^0$	27.7 ± 2.7	23.2 ± 2.2		18.6 ± 0.9	0.1
$K_{\mu 3} \rightarrow \mu^+ + \pi^0 + \nu$	2.8 ± 1.0	5.9 ± 1.3	2.8 ± 0.4	4.8 ± 0.6	0.3
$K_{e3} \rightarrow e^+ + \pi^0 + \nu$	3.2 ± 1.3	5.1 ± 1.3		5.0 ± 0.5	0.0
$\tau^+ \rightarrow 2\pi^+ + \pi^-$	5.6 ± 0.4	6.8 ± 0.4	5.2 ± 0.3	5.7 ± 0.3	0.0
$\tau^{+\prime} \rightarrow \pi^+ + 2\pi^0$	2.1 ± 0.5	2.2 ± 0.4	1.5 ± 0.2	1.7 ± 0.2	0.1

[a] See reference 1.
[b] See reference 2.
[c] See reference 3.

between π and μ secondaries on the basis of observed π-μ decays. Since most K^+ mesons stop near the center of the chamber, the 24-cm range of the π^+ from the $K_{\pi 2}{}^+$ decay mode is too long in a 30-cm diameter chamber to be useful as a method of separation of $K_{\pi 2}$ from other modes.

We now illustrate in a slightly oversimplified way the method of calculating the branching ratios from the data. We let $N_1, N_2, \cdots N_7$ denote the numbers of events in the above seven categories, and let $N = \sum_i N_i$. We also define $C(K_i, j)$ as the probability that in the decay mode K_i, j gamma rays are converted and observed in the appropriate fiducial volume of the bubble chamber, e.g., $C(K_{\mu 3}, 1)$ is the probability of observing one gamma ray from a $K_{\mu 3}$. Finally we let C_e be the probability of recognition of an electron, by virtue of its large energy loss or production of a shower in the chamber. In terms of the above quantities, the branching ratios can be calculated from the following relations:

$$B(\tau) = N_1/N,$$

$$B(\tau') = \frac{N_2}{N[C(\tau', 4) + C(\tau', 3)]},$$

$$B(K_{e3}) = N_3/C_e N,$$

$$B(K_{\mu 3}) = \frac{1}{C(K_{\mu 3}, 2)}[N_5/N - C(\tau', 2)B(\tau') - B(K_{e3})(1 - C_e)C(K_{e3}, 2)],$$

$$B(K_{\pi 2}) = \frac{1}{C(K_{\pi 2}, 2) + C(K_{\pi 2}, 1)}[(N_4 + N_6)/N - C(\tau', 1)(B(\tau') - C(K_{\mu 3}, 1)B(K_{\mu 3}) - (1 - C_e)C(K_{e3}, 1)B(K_{e3})],$$

$$B(K_{\mu 2}) = N_7/N - C(\tau', 0)B(\tau') - C(K_{\mu 3}, 0)B(K_{\mu 3}) - C(K_{\pi 2}, 0)B(K_{\pi 2}) - (1 - C_e)C(K_{e3}, 0)B(K_{e3}).$$

The determination of the efficiencies $C(K_i, j)$ consists of two parts: computation of the conversion probabilities in the chamber, and estimation of the fraction of electron pairs missed because of scanning inefficiency. The first part was done by a Monte Carlo technique in which the observed spatial distribution of K^+-decay points and the theoretical gamma-ray conversion cross section were used to compute the probabilities of forming various numbers of electron pairs within the appropriate fiducial volume. These efficiencies are insensitive to assumptions about π^0 momentum distributions in the three-body decay modes and are approximately represented by multinomial distributions with conversion probability of 80% for a single gamma ray. From the Monte Carlo calculation, we find that the fraction of $K_{\pi 2}$ events in which neither gamma ray from the π^0 converts is only 5%.

The effects of scanning inefficiency were minimized in the following ways: (a) All pictures were scanned twice by technicians or physicists. (b) About 30% of the pictures were scanned independently by two physicists. (c) Only pictures of the best quality, without too many K^+ mesons, were used in the analysis. (d) All K^+-decay points were required to fall within an appropriate fiducial volume appreciably smaller than the bubble chamber.

An important check on the efficiency was afforded by a comparison of the experimentally found relative proportion of events with one and with two electron pairs and those obtained by the Monte Carlo computation. From this comparison, we conclude that the average scanning efficiency for electron pairs is $(85 \pm 2)\%$. Much of this loss can be ascribed to steeply dipping and low-energy pairs. An error of 2% in the efficiency estimate would change the branching ratios by the amounts shown in the last column of Table I.

The electron recognition efficiency C_e was obtained by measuring, for a sample of identified K_{e3} events, both the minimum amount of track required to identify the electron and its potential path length in the chamber. From these data, the electron recognition probability as a function of potential path was evaluated and, averaged over the potential path distribution, yielded $C_e = (89 \pm 2.5)\%$.

Small corrections were applied to the results obtained as described above for the following effects: (a) the presence of a small contamination of decays in flight, for which the kinematical $K_{\pi 2}$ tests discussed previously are incorrect; (b) the fact that, because of measurement errors, a small number of $K_{\mu 3}$ events pass the $K_{\pi 2}$ kine-

matical tests.

The final results are given in Table I, which for comparison also contains the results of emulsion determinations by Birge et al., Alexander et al., and Taylor et al.

No clear example of a decay mode other than the six considered above was found, but it must be emphasized that no systematic search aimed specifically at the identification of rare modes has yet been completed.

We wish to express our appreciation to Dr. J. D. Van Putten and Dr. H. C. Bryant, and to the staff of the Bevatron for their invaluable help in the course of this experiment.

*This work was done under the auspices of the U. S. Atomic Energy Commission.

†Now at Physics Department, University of California, Berkeley, California.

[1]R. W. Birge, D. H. Perkins, J. E. Peterson, D. H. Stork, and M. W. Whitehead, Nuovo cimento 4, 834 (1959).

[2]G. Alexander, R. H. W. Johnston, and C. O'Ceallaigh, Nuovo cimento 6, 478 (1957).

[3]S. Taylor, G. Harris, J. Orear, J. Lee, and P. Baumel, Phys. Rev. 114, 359 (1959).

[4]J. L. Brown, H. C. Bryant, R. A. Burnstein, D. A. Glaser, R. Hartung, J. A. Kadyk, J. D. Van Putten, D. Sinclair, G. H. Trilling, and J. C. Van der Velde, Nuovo cimento 19, 1155 (1961).

INTERACTIONS OF LAMBDAS WITH PROTONS*

Gideon Alexander,† Jared A. Anderson, Frank S. Crawford, Jr., William Laskar, and Lester J. Lloyd

Lawrence Radiation Laboratory, University of California, Berkeley, California

(Received September 29, 1961)

In the course of an experiment to study the associated production processes,

$$\pi^- + p \rightarrow \Lambda + K^0 \quad (1)$$

and

$$\pi^- + p \rightarrow \Sigma^0 + K^0, \quad \Sigma^0 \rightarrow \Lambda + \gamma, \quad (2)$$

we have examined subsequent Λ interactions in hydrogen of the types

$$\Lambda + p \rightarrow \Lambda + p, \quad (3)$$

$$\Lambda + p \rightarrow \Sigma^0 + p, \quad (4)$$

$$\Lambda + p \rightarrow \Sigma^+ + n. \quad (5)$$

In this Letter we present results for reactions (3) and (4), based on a sample of 5000 Λ's produced in the Alvarez 72-in. hydrogen bubble chamber. [We postpone discussion of reaction (5) to a later publication.] In addition, we set an upper limit to the pion-producing reactions,

$$\Lambda + p \rightarrow \Lambda + p + \pi^0$$

and

$$\Lambda + p \rightarrow \Lambda + n + \pi^+. \quad (6)$$

The Λ "beam" momentum extends from 400 to 1000 Mev/c, and corresponds to the associated production processes (1) and (2) for incident π^-'s of 1035 Mev/c. The distribution of Λ momentum versus path length is shown in Fig. 1. It includes two cutoff corrections: (a) Single V^0 decays of K^0 or Λ (without subsequent scatter) are rejected if the neutral particle travels less than 0.5 cm before decaying; (b) only those Λ interactions that occur within 10 cm of the production point are accepted. Cutoff (a) serves to exclude spu-

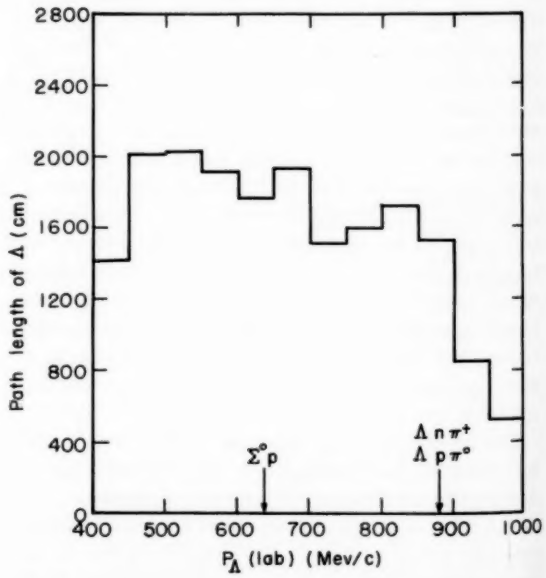

FIG. 1. Distribution of Λ path length versus momentum. The arrows indicate the thresholds for reactions (4) and (6).

rious V^0's due to two-prong events. Cutoff (b), while including most of the Λ path length before decay, serves to minimize the geometrical escape correction, and helps to exclude random background recoil protons from candidacy.

Lambda interactions that are followed by the charged decay $\Lambda \to p + \pi^-$ are detectable whether or not the associated K^0 undergoes charged decay. Interactions followed by the neutral decay $\Lambda \to n + \pi^0$ are also detectable and are used, provided that the K^0 decays via the charged mode. The kinematics and measuring errors are such that there is no difficulty in distinguishing between reactions (3) and (4).

Some of the interactions were found by scanners in the first scan. However, the main search for interactions consisted of (a) a systematic examination on the scanning table of all single and double V^0 events which failed to satisfy the kinematics for production via reactions (1) and (2), and (b) an examination on the scanning table of all single V^0 events where the decaying neutral is identified as a K^0. Here one looks for a recoil proton starting from the line of flight of the Λ.

Recoil protons of less than 0.5 cm are difficult to detect, and have been excluded. Our elastic-scattering cross section [Reaction (3)] therefore does not include small-angle scatters of the Λ. The excluded angular region depends on the momentum of the incident Λ, and is indicated by the shaded region in Fig. 2.

The correction to the integrated cross section depends on the shape of the angular distribution. The elastic-scattering cross sections include a cutoff correction for which uniformity in $\cos\theta_\Lambda$ (c.m.) and P_Λ (lab) is assumed. From Fig. 2 we see that, within the limited statistics, these assumptions are satisfied. The correction factor amounts to 1.074 for P_Λ(lab) from 400 to 638 Mev/c, and 1.028 for P_Λ(lab) above 638 Mev/c, the threshold for $\Sigma^0 - p$ production.

In the cases of the endothermic processes (4), (5), and (6), the proton range exceeds 0.5 cm for all production angles over the entire range of P_Λ(lab), so that there is no corresponding cutoff correction.

Details of the individual events are found in Table I. Figure 2 shows the laboratory momentum of the incident Λ and the c.m. angle of the final hyperon (relative to the incident Λ) for each event. Table II gives our cross-section results. The elastic-scattering cross section is given for the entire momentum interval, and separately for the intervals below and above 638 Mev/c, the threshold for reaction (4). The upper limit given for the pion-producing reaction (6) is the cross section that would correspond to finding a single event instead of the number (zero) actually found.

Our elastic-scattering cross section can be compared with the previous result of Crawford et al.,[1] obtained in substantially the same momentum interval. Based on four events, they found a cross section of 40 ± 20 mb, which is not in disagreement with our result of 22.3 ± 5.9 mb.

Information from study of hyperfragments has been used by Kovacs and Lichtenberg[2] to calculate the elastic-scattering cross section at 416 Mev/c (75 Mev) and at 598 Mev/c (150 Mev). They chose a phenomenological central potential with a hard core and considered only angular momenta of ≤ 2. Their calculated results are 26 and 21 mb at 416 and 598 Mev/c, respectively, when no spin-orbit term is included, and 34 and 32 mb

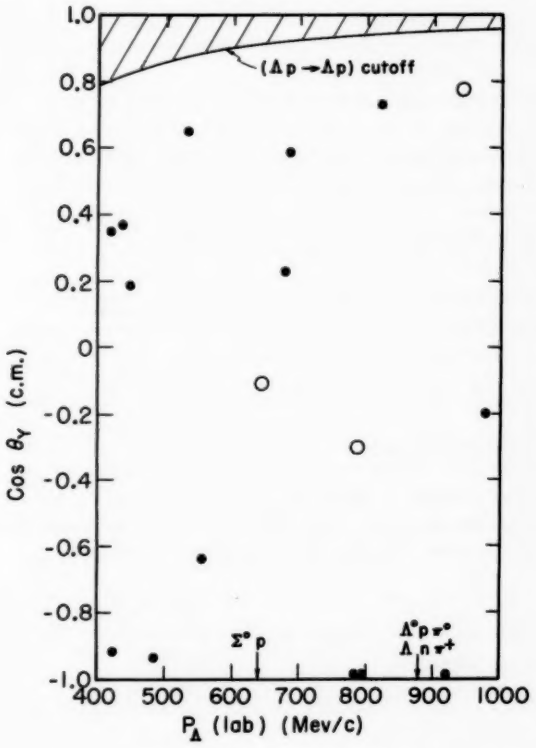

FIG. 2. Details of the interactions. Solid circles indicate elastic scattering events [reaction (3)]. Open circles represent Σ^0-p production [reaction (4)]. The shaded region corresponds to elastic scattering in which the recoil proton has a range of <5 mm.

Table I. Details of the interactions.

Frame	Initial lab momentum of Λ (Mev/c)	Center-of-mass momentum Initial	Final	$\cos\theta_Y$(c.m.)
	A. $\Lambda+p\rightarrow\Lambda+p$			
602 103	418	188	188	+0.35
722 504	421	189	189	−0.92
739 246	436	196	196	+0.37
865 515	447	200	200	+0.19
818 550	483	216	216	−0.94
586 135	532	236	236	+0.65
537 508	555	246	246	−0.64
834 420	678	297	297	+0.23
864 246	684	300	300	+0.58
814 534	787	341	341	−0.99
602 317	796	345	345	−0.99
857 282	822	355	355	+0.73
539 021	921	393	393	−0.99
724 478	977	413	413	−0.20
	B. $\Lambda+p\rightarrow\Sigma^0+p$			
861 205	646	284	42	−0.11
586 381	788	341	193	−0.30
692 127	943	401	285	+0.78

when spin-orbit interaction is included. Our measured value of 24.7 ± 9.3 mb for the interval 400 to 638 Mev/c is compatible with either calculated result. Thus we agree with the prediction from hyperfragment data, but cannot distinguish between the presence or absence of spin-orbit terms.

In the doublet approximation (DA),[3] the $\Sigma-\Lambda$ mass difference is neglected and $\Sigma^{\pm,0}$ and Λ are combined into the two doublets,

$$N_2=[\Sigma^+,\ (\Lambda-\Sigma^0)/\sqrt{2}\,]\ \text{and}\ N_3=[(\Lambda+\Sigma^0)/\sqrt{2},\ \Sigma^-].$$

Both N_2 and N_3 have the same coupling to the pion field. This pion coupling need not be the same as that of the nucleon doublet $N_1=[p,\ n]$. In addition, a new quantum number is introduced which prevents mixing of the doublets.[3] (For instance, $\Sigma^-+p\rightarrow\Sigma^++n+\pi^-$ is forbidden in DA.) The mass difference between N_2 or N_3 and the nucleon N_1 is not neglected.

One can then show that

$$2[\sigma(\Lambda p\rightarrow\Lambda p)+\sigma(\Lambda p\rightarrow\Sigma^0 p)]$$
$$=\sigma(\Sigma^+p\rightarrow\Sigma^+p)+\sigma(\Sigma^-p\rightarrow\Sigma^-p). \qquad (7)$$

Of course, Eq. (7) can only be valid at energies high enough that the actual $\Sigma-\Lambda$ mass difference is negligible compared with the c.m. kinetic energy. For instance, Eq. (7) is certainly inapplicable below threshold for $\Lambda p\rightarrow\Sigma^0 p$. As a first approximation to a test of Eq. (7), we compare our results for the reactions on the left side of Eq. (7) to those of Stannard[4] for those on the right side. We consider the $\Lambda p\rightarrow\Lambda p$ cross section only

Table II. Summary of cross-section results.

Reaction	P_Λ(lab) (Mev/c)	No. of events	Λ path length (cm)	Cross section (mb)
$\Lambda+p\rightarrow\Lambda+p$	400-1000	14	18 770	22.3 ± 5.9
$\Lambda+p\rightarrow\Lambda+p$	400- 638	7	8700	24.7 ± 9.3
$\Lambda+p\rightarrow\Lambda+p$	638-1000	7	10 070	20.4 ± 7.7
$\Lambda+p\rightarrow\Sigma^0+p$	638-1000	3	10 070	8.5 ± 4.9
$\Lambda+p\rightarrow\begin{Bmatrix}\Lambda+p+\pi^0\\ \Lambda+n+\pi^+\end{Bmatrix}$	880-1000	0	1986	$<14\pm14$

for P_Λ(lab) above 638 Mev/c, the threshold for reaction (4). Our range of total c.m. energy corresponds to a Σ-p c.m. momentum range of 0 (at threshold) to 314 Mev/c [for P_Λ(lab) of 1000]. Stannard's results correspond to a Σ-p c.m. momentum range of 0 to about 600 Mev/c.

We find

$$2[\sigma(\Lambda p \to \Lambda p) + \sigma(\Lambda p \to \Sigma^0 p] = 57 \pm 18 \text{ mb}.$$

Stannard finds

$$\sigma(\Sigma^+ p \to \Sigma^+ p) + \sigma(\Sigma^- p \to \Sigma^- p) = 48 \pm 17 \text{ mb}.$$

Within the statistical errors, the prediction [Eq. (7)] of the doublet approximation is well satisfied.

In the theory of global symmetry (GS),[5] the assumption (in addition to those of DA) is made that the pion coupling of N_2 and N_3 is the same as that of the nucleon N_1, and the mass difference between N_2 or N_3 and N_1 is neglected. One can then predict N_1-N_2 or N_1-N_3 interactions from N_1-N_1 (nucleon-nucleon) interactions. de Swart and Dullemond have used potentials that fit available nucleon-nucleon scattering data, in linear combinations prescribed by GS, to predict cross sections for hyperon-nucleon interactions.[6] They take exactly into account the Σ-Λ mass difference in the kinematics (but neglect the Σ-nucleon mass difference). Their predictions for Λ-p elastic scattering and for Σ^0-p production [reaction (4)] are shown in Fig. 3, together with our experimental results. Within statistics, our cross sections agree with the predictions of GS.

de Swart and Dullemond also predict angular distributions for Λ-p elastic scattering at 475, 640, and 815 Mev/c. These momenta cover our range of P_Λ fairly well (see Fig. 1). With our limited statistics we can check at most a single parameter of the angular distribution. We examine our ratios for forward-to-backward scattering (F/B) and for polar-to-equatorial scattering (P/E). Since we see no strong momentum dependence in the elastic-scattering cross section, and since the predicted angular distributions do not vary drastically over our momentum range, we average with equal weight the theoretical predictions for F/B and P/E and compare them with our entire sample of 14 events.

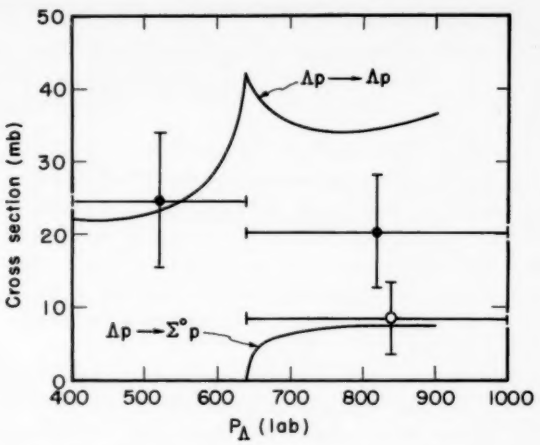

FIG. 3. Comparison of our experimental results with the predictions (based on global symmetry) of de Swart and Dullemond.[6] The upper curve and the solid circles represent elastic scattering. The lower curve and open circle correspond to Σ^0-p production.

For F/B we find $7/7 = 1.0 \pm 0.5$. The prediction of GS is 1.5.

For P/E we find $9/5 = 1.8 \pm 1.0$. The GS prediction is 2.0.

It is a pleasure to acknowledge the guidance and encouragement of Professor Luis W. Alvarez.

---

*This work was done under the auspices of the U. S. Atomic Energy Commission.

†International Cooperation Administration Fellow on leave of absence from the Israel Atomic Energy Commission Laboratories, Rehovoth, Israel.

[1]F. S. Crawford, M. Cresti, M. L. Good, F. T. Solmitz, M. L. Stevenson, and H. K. Ticho, Phys. Rev. Letters 2, 174 (1959).

[2]J. S. Kovacs and D. B. Lichtenberg, Nuovo cimento 13, 371 (1959).

[3]A. Pais, Phys. Rev. 110, 574 (1958); Lawrence Radiation Laboratory Report UCRL-9460, 1960 (unpublished); Nuovo cimento 18, 1003 (1960).

[4]F. R. Stannard, Phys. Rev. 121, 1513 (1961).

[5]E. P. Wigner, Proc. Natl. Acad. Sci. U. S. 38, 449 (1952); J. Schwinger, Ann. Phys. 2, 407 (1957); M. Gell-Mann, Phys. Rev. 106, 1296 (1957).

[6]J. J. de Swart and C. Dullemond, University of Rochester Report NYO-9746, 1961 [Ann. Phys. (to be published)].

$\pi^+ + p$ AND $\pi^- + p$ TOTAL CROSS SECTIONS FROM 8 TO 20 Bev/c*

S. J. Lindenbaum, W. A. Love, J. A. Niederer, S. Ozaki, J. J. Russell, and L. C. L. Yuan
Brookhaven National Laboratory, Upton, New York
(Received October 12, 1961)

Previous experiments[1,2] by von Dardel et al. have reported measurements of the $\pi^+ + p$ and $\pi^- + p$ total cross sections over the incident pion momentum range of 4-10 Bev/c. These investigators have found that both the $\pi^+ + p$ and $\pi^- + p$ total cross sections decrease slowly and monotonically (by $\approx 10\%$) going from 4.5 Bev/c to 10 Bev/c incident pion momentum.

At 10 Bev/c, $\sigma_t(\pi^- + p) = 27.0 \pm 0.4$ mb, $\sigma_t(\pi^+ + p) = 25.2 \pm 0.4$ mb, and $\sigma_t(\pi^- + p) - \sigma_t(\pi^+ + p) = 1.8 \pm 0.6$ mb, where the subscript t denotes total cross section. As those authors concluded, the data do not satisfy the necessary conditions for application of the Pomeranchuk theorem[3] which is that both $\sigma_t(\pi^+ + p)$ and $\sigma_t(\pi^- + p)$ become and remain constant with increasing energy. As a matter of fact, neither cross section appears to be consistent with this condition.

In a recent publication[4] the authors of this communication have investigated the antiproton-proton and the proton-proton total cross section from 4 to 20 Bev/c. $\sigma_t(p + p)$ appeared to become and remain constant within the errors from 10 to 20 Bev/c [$\sigma_t(p+p) \approx 39.5 \pm 1$ mb], but the total antiproton-proton cross section continued to decrease monotonically from 10 Bev/c where $\sigma_t(\bar{p} + p) = 58 \pm 4$ mb to 20.3 Bev/c where $\sigma_t(\bar{p} + p) = 48 \pm 4$ mb, and hence the Pomeranchuk theorem could not be verified by this investigation. Therefore it appeared to be of considerable interest to extend the investigation of the $\sigma_t(\pi^- + p)$ and the $\sigma_t(\pi^+ + p)$ to the so far uninvestigated energy range of 10-20 Bev/c. The $\pi^- - \pi^+$ particle-antiparticle pair is especially interesting to compare since, in addition to the general Pomeranchuk theorem,[5] there is another specific argument which can be applied to the behavior of the difference $\sigma_t(\pi^- + p) - \sigma_t(\pi^+ + p)$ at high enough energies which cannot be applied to the behavior of the difference $\sigma_t(\bar{p} + p) - \sigma_t(p + p)$ or the difference $\sigma_t(K^- + p) - \sigma_t(K^+ + p)$. This argument, which was proposed by Okun and Pomeranchuk,[6] can be summarized as follows. At high enough energies one would expect the charge-exchange cross section to become small compared to the total inelastic cross section, since charge exchange represents only one inelastic channel of what one might expect to be an arbitrarily large number of possible inelastic channels at sufficiently high energy. Therefore the $T = \frac{3}{2}$ state complex scattering amplitude must approximately equal the $T = \frac{1}{2}$ state complex scattering amplitude, since the charge-exchange amplitude is proportional to the difference of these two amplitudes. This then implies that the $\pi^- + p$ total elastic scattering cross section equals the $\pi^+ + p$ total elastic scattering cross sections and hence also that

$$\sigma_t(\pi^- + p) = \sigma_t(\pi^+ + p).$$

Of course the above argument does not depend on the constancy of cross sections at high energy which is a necessary requirement for the Pomeranchuk theorem, and also does not depend on the validity of the forward dispersion relations which are employed to prove the theorem.

Weinberg[7] has recently presented a generalized Pomeranchuk theorem which relaxes the conditions required to prove that $\sigma_+ - \sigma_- \to 0$ as $E \to \infty$; σ_+ is the particle total cross section and σ_- is the antiparticle total cross section. The essential assumptions are: (a) that the difference $\sigma_+(E) - \sigma_-(E)$ does not change sign an infinite number of times; (b) that the cross sections $\sigma_\pm$ do not grow faster than $(\ln E)^{1/2}$ as $E \to \infty$. Then, using the forward dispersion relations, he demonstrates that $\sigma_+ - \sigma_- \to 0$ as $E \to \infty$.

The present experiment to determine $\sigma_t(\pi^+ + p)$ and $\sigma_t(\pi^- + p)$ from 8 to 20 Bev/c was run during the same period and with the same experimental arrangement as the previously reported work on $\sigma_t(\bar{p} + p)$ and $\sigma_t(p + p)$,[4] the only difference being that the gaseous Čerenkov counter was tuned to a pressure which selected pions rather than protons, or antiprotons. The previous method of using six counters of different area to extrapolate the measured transmission to zero area was again employed. The measured transmissions and hence also the values of the cross sections were corrected for the following effects:

(a) Due to the π-μ and K-μ_2 decays there is a muon contamination of the beams. Using the known pion and K-meson production spectra and angular distributions from previous work,[8] the known K-meson and pion lifetimes, and the beam setup geometry and magnetic geometry, we were able to estimate the muon contamination of the pion beam to range from 2 to 3%, with an error of $\pm 1\%$; this correction was applied to the data. The uncertainty in the difference of $\sigma_t(\pi^- + p) - \sigma_t(\pi^+ + p)$

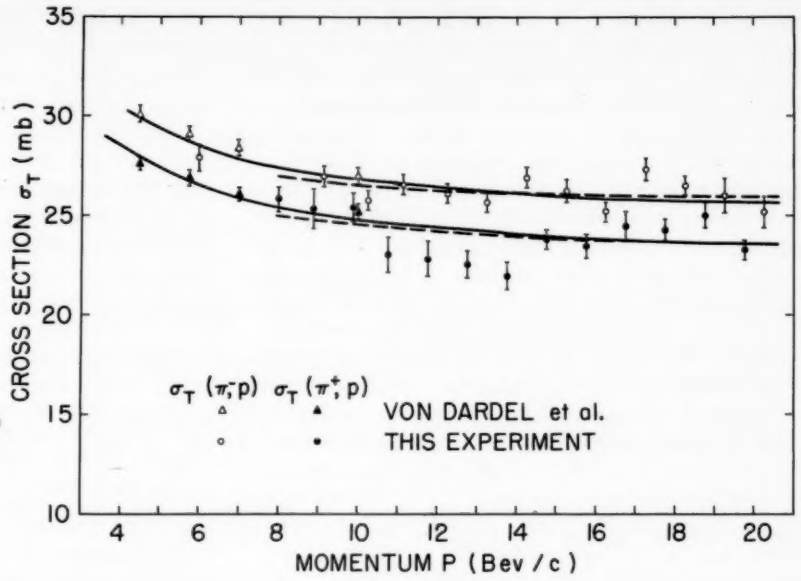

FIG. 1. $\pi^- + p$ and $\pi^+ + p$ total cross sections. The solid lines are Fit 2′ and the dashed lines are Fit 2 (see text). The momentum of the system is defined to ~±2.5%, and the absolute scale of the momentum is uncertain by 2%.

due to muon contamination is only a fraction of a percent.

(b) The electron contamination of the beam was estimated to be ~0.3% and a correction was made.

(c) Accidentals mainly in the end counter array were monitored during the run and the appropriate correction (~1%) to the cross sections was made with an uncertainty of a fraction of 1%.

(d) The proton contamination correction to the cross section is less than 1% below 15 Bev/c and rises to approximately 3.5% at 20 Bev/c. The uncertainty in the cross section due to this correction is less than 1%.

The results are shown in Fig. 1. The errors on each point predominantly represent point-to-point errors. In addition we estimate that the absolute scale uncertainty may be as much as 2% (i.e., 0.5 mb); however, this absolute uncertainty has a negligible effect on the difference $\sigma_t(\pi^- + p) - \sigma_t(\pi^+ + p)$.

From Fig. 1 it is clear that our results agree very well with those of von Dardel et al. at the lower momenta. Considering the errors, it appears that there is no convincing evidence from the present data for other than a smooth slow variation of the total cross section with energy. Therefore we have attempted three least-squares fits of the momentum dependence of the total cross sections from 8 to 20 Bev/c. Fit 1: $\sigma_t = a$; Fit 2: $\sigma_t = a + b/p$; Fit 3: $\sigma_t = a + b/\ln p$; where both a and b are constants. It was found that Fit 2 has the lowest χ^2, and on inspection of the lower energy data of von Dardel et al. it appears that Fit 2 and Fit 3 are the only fits capable of reasonably fitting the data from 4.5 to 20 Bev/c.

Fit 2′ is the Fit 2 momentum dependence $\sigma_t = a + b/p$ but applied to the sum of our data and the data of von Dardel et al. (i.e., a fit from 4.5 to 20 Bev/c). Both Fit 2 and Fit 2′ are shown in Fig. 1. It is clear that this functional dependence can be made to fit both our own and the lower energy data reasonably well. The parameters a and b for these fits are given in Table I.

The calculated differences $\Delta = \sigma_t(\pi^- + p) - \sigma_t(\pi^+ + p)$

Table I. Fit of $\sigma_t = a + b/p$, where σ_t is in mb and p is pion lab momentum in Bev/c.

	Fit 2		Fit 2′	
σ_t	a	b	a	b
$\sigma_t(\pi^+ + p)$	22.59 ± 0.63	19.39 ± 8.21	22.26 ± 0.33	25.10 ± 2.83
$\sigma_t(\pi^- + p)$	25.26 ± 0.46	13.03 ± 5.27	24.37 ± 0.29	24.94 ± 2.65

for all of the fits 1, 2, 2′, and 3 show that Δ is probably constant or at best slowly decreasing from 4.5 to 20 Bev/c. On the other hand, the total cross sections decrease monotonically by about 10% from 4.5 Bev/c to 10 Bev/c, and the additional decrease from 10 Bev/c to 20 Bev/c is only about 4%. If the assumed functional dependence $\sigma = a + b/p$ were to be correct for higher energies, our results imply that the limiting values of both total cross sections at very high energies would decrease from the values at 20 Bev/c by about 5% but the same order of difference ($\Delta \sim 2$ mb) would still remain. We also found this to be the case for the other fits.

Although extrapolation of the observed momentum dependence of the cross section in the observed energy range to much higher energies is not to be taken very seriously, it is, on the other hand, strongly implied by our data that at 20 Bev/c we are still very far from the energy region where the Pomeranchuk or Weinberg theorems, etc., can be applied or even apparently verified. Furthermore the substantial difference $\sigma_t(\pi^- + p) - \sigma_t(\pi^+ + p)$ and its slow decrease with energy that we have observed also imply that the number of inelastic channels which are effective is much too small and is growing much too slowly with energy to allow us to believe that we are approaching the necessary energy to demonstrate the high-energy limit theorems considered.

In view of our previous work on antiproton-proton and proton-proton total cross sections[1] and other previous work on K^+-proton and K^--proton total cross sections, we now believe that it is likely that even a possible experimental verification of the high-energy limit theorems (i.e., $\sigma_+ - \sigma_- \to 0$ as $E \to \infty$) will have to await the next large increase in proton accelerator energy.

The authors wish to acknowledge the cooperation of the AGS staff and the operating crew during these experiments. The authors also wish to acknowledge the assistance of J. Elias and C. Sinclair during these experiments.

---

*This work was performed under the auspices of the U. S. Atomic Energy Commission.

[1]G. von Dardel, D. H. Frisch, R. Mermod, R. H. Milburn, P. A. Piroué, M. V. Vivargent, G. Weber, and K. Winter, Phys. Rev. Letters 5, 333 (1960).

[2]G. von Dardel, R. Mermod, P. A. Piroué, M. V. Vivargent, G. Weber, and K. Winter, Phys. Rev. Letters 7, 127 (1961).

[3]I. Pomeranchuk, J. Exptl. Theoret. Phys. (U.S.S.R.) 34, 725 (1958) [translation: Soviet Phys. – JETP 34(7), 499 (1958)].

[4]S. J. Lindenbaum, W. A. Love, J. A. Niederer, S. Ozaki, J. J. Russell, and L. C. L. Yuan, Phys. Rev. Letters 7, 185 (1961).

[5]From Pomeranchuk's theorem, one concludes that if $\sigma_t(\pi^+ + p)$ and $\sigma_t(\pi^- + p)$ become and remain constant beyond an energy $E > \epsilon$ then $\sigma_t(\pi^+ + p) = \sigma_t(\pi^- + p)$ for $E > \epsilon$.

[6]L. B. Okun and I. I. Pomeranchuk, J. Exptl. Theoret. Phys. (U.S.S.R.) 30, 424 (1956) [translation: Soviet Phys.–JETP 3, 307 (1956)].

[7]S. Weinberg, Phys. Rev. (to be published).

[8]W. F. Baker, R. L. Cool, E. W. Jenkins, T. F. Kycia, S. J. Lindenbaum, W. A. Love, D. Luers, J. A. Niederer, S. Ozaki, A. L. Read, J. J. Russell, and L. C. L. Yuan, Phys. Rev. Letters 7, 101 (1961).

EXISTENCE OF TWO $T=0$ VECTOR MESONS*

J. J. Sakurai
The Enrico Fermi Institute for Nuclear Studies and the Department of Physics,
University of Chicago, Chicago, Illinois

(Received October 12, 1961)

We wish to interpret the various recently discovered vector meson states within the framework of the vector theory of strong interactions[1,2] (VTSI) proposed nearly two years ago. In particular, we concentrate our attention on the two distinct $T=0$ vector mesons unambiguously predicted by VTSI. The following are some of the major points we would like to make:

(1) The 550-Mev peak in the $\pi^+\pi^-\pi^0$ mass plot for the reaction

$$\pi^+ + d \to \pi^+ + \pi^- + \pi^0 + 2p$$

studied by the Johns Hopkins–Northwestern group[3] may well be due to a second $T=0$ vector meson state (tentatively called η^0) with exactly the same quantum numbers as the experimentally well established ω^0 at 785 Mev.

(2) In the language of VTSI, the ω^0 is to be identified with the vector meson coupled to the baryonic current whereas the η^0 with a lower mass is to be identified with the vector meson coupled to the hypercharge current.

(3) Most of the hard-core effect between two nucleons should come from the exchange of an ω^0 rather than from the exchange of an η^0.

(4) The conjectured η with a mass lower than the ρ ($T=1$, $J=1-$ two-pion resonance) mass is extremely helpful in understanding the nucleon structure.

(5) Generalized Clementel-Villi-Fubini type analyses applied to the observed nucleon form factors suggest that 120% of the isoscalar charge is due to η, and that 120% of the isovector charge is due to ρ; hence, using the argument of Gell-Mann and Zachariasen,[4] we infer that the universality relations implied by the couplings of the vector mesons to the appropriate conserved currents may hold approximately even at $s=m_\rho{}^2$, $m_\eta{}^2$.

Some time ago a theory of strong interactions was proposed which unambiguously predicts the existence of one $T=1$ vector meson (p-wave two-pion resonance) and two $T=0$ vector mesons ($T=0$, $J=1-$ three-pion resonances). Recent πN and $\bar{p}p$ experiments[5,6] have conclusively established that there indeed exist a $T=1$ vector meson ρ with a mass of 750 Mev and a width of ~80 Mev and a $T=0$ vector meson ω^0 with a mass of 785 Mev and a width <30 Mev. Moreover, Pevsner and collaborators[3] report that, in the reaction

$$\pi^+ + d \to \pi^+ + \pi^- + \pi^0 + 2p, \qquad (1)$$

in addition to the clearly identified ω^0 peak (whose mass agrees well with that of Maglić et al.[6]), there is an indication for another peak in the Q-value plot for $\pi^+\pi^-\pi^0$ which might be associated with a three-pion resonance with a mass of ~550 Mev and a width <30 Mev. The statistics are still meager, and the effect may disappear later.[7] Neither the isospin nor the spin-parity assignment has been made. Yet in the present note we take this state seriously, and call it η^0. Moreover, we assume that η^0 is a $T=0$ vector meson that decays strongly into three pions with $T=0$, $J=1-$, just like ω^0. (As the η mass is not far above the three-pion threshold, the two-body electromagnetic decay mode $\pi^0+\gamma$ might also be detectable; if we use the method of Gell-Mann and Zachariasen[4] to compute the decay rate for $\eta^0 \to \pi^0+\gamma$ from the π^0 lifetime, we obtain about 0.03 Mev for the partial width provided that $f_\eta{}^2/4\pi \sim 2$.)

Let us recall that the two $T=0$ vector mesons of VTSI are coupled linearly to the two exactly conserved $T=0$ currents of the strong interactions—the hypercharge current and the baryonic current. The following question naturally arises: Is $\omega^0(\eta^0)$ coupled to the baryonic current or to the hypercharge current? Note that here we have two particles or resonant states that have identical isospins and identical spin parities; moreover, their widths seem narrow in both cases. The only difference is that the ω mass is 230 Mev higher than the η mass. Yet according to VTSI, their roles in strong-interaction physics are quite distinct. For instance, if the pseudoscalar mesons, π and K, are to emerge as tightly bound states of $N\bar{N}$ and $N\bar{\Lambda}$ systems, glued by a heavy neutral vector meson as suggested by Teller and others,[1,8] the coupling of the baryonic vector meson ($B^{(B)}$ of reference 1) must be much stronger than the coupling of the hypercharge vector meson ($B^{(Y)}$ of reference 1); otherwise there would be a very tightly bound state of a $\bar{K}$ and an N.

In principle, it is possible to settle this question by studying the analytic structure of the KN

scattering amplitudes as functions of momentum transfer. For instance, if η^0 (but not ω^0) is the vector meson coupled to the hypercharge current, both the $T=1$ KN amplitude and the $T=0$ KN amplitude must have poles at $t=m_\eta{}^2$ with equal residues, but no poles should be present at $t=m_\omega{}^2$. In practice, however, this will not be feasible for a long time to come. A more practical way is to study the effects of η^0 and ω^0 on nuclear forces at short distances, keeping in mind that the coupling of the baryonic vector meson to the nucleon must be much stronger than the coupling of the hypercharge vector meson to the nucleon. Just as the baryonic vector meson is responsible for most of the attraction necessary to bind a baryon and an antibaryon to form a π or a K, the same particle must also be responsible for most of the observed short-ranged, very strong repulsion between two nucleons. In this connection we should recall an important observation made by Breit,[9] who also advocated the neutral-vector-meson approach to nuclear forces to account for the repulsive core and the spin-orbit force in a unified manner.[10] He demonstrates that with a vector coupling constant of the order of 10 and with a vector meson mass $\sim 4m_\pi$, the repulsive core radius would become too large in the sense that the central force in the intermediate region (distance $\sim 0.75/m_\pi$) would be completely dominated by the strong repulsion due to the vector meson. Although a rigorously quantitative discussion of Breit's argument must await a more reliable estimate of the two-pion exchange contribution to nuclear forces than is now available, there is no doubt that between ω with $m_\omega = 5.9\,m_\pi$ and η with $m_\eta = 4.0\,m_\pi$, the ω is the more likely candidate for the $T=0$ vector meson coupled strongly to the baryonic current. In the language of reference 1, this means that ω^0 is the vector meson associated with the $B_\mu^{(B)}$ field while η^0 is the one associated with the $B_\mu^{(Y)}$ field.[11]

It is encouraging that, in both $p\bar{p}$ collisions and $\pi^+ d$ collisions, ω mesons show up much more conspicuously than η mesons. In reaction (1) at $p_\pi^{(\mathrm{lab})} = 1.23$ Bev/c, the cross section for ω^0 production seems to be about four times as large as that for η^0 production.[3] In $p+\bar{p} \to 5\pi$, 7π, there is hardly any evidence for η's.[8] Thus, contrary to Chew and Frautschi,[12] all strong interactions do not seem as strong as possible; rather some strong couplings such as the coupling of ω^0 to $N\bar{N}$ seem much stronger than other strong couplings such as the coupling of η^0 to $N\bar{N}$, as conjectured earlier.[1]

We now examine the nucleon structure problem in the light of the existence of ρ, η, and ω. Electron-proton scattering experiments carried out at Stanford and Cornell[13] have revealed that the neutron charge cloud has a fairly large positively charged "fringe." In a more sophisticated language, the average mass state responsible for the isoscalar form factor must be lower than that responsible for the isovector form factor. Applying Clementel-Villi[14] type fits to the nucleon form factors, it was concluded by Bergia et al.[15] (BSFV) that, if a simple resonance picture (which has its origin in the pioneer work of Nambu[16]) holds, the $T=1$, $J=1-$ two-pion resonance proposed by Frazer and Fulco[17] must have a higher mass than the $T=0$, $J=1-$ three-pion resonance proposed by Nambu[16] and Chew.[18] Thus the simple resonance picture of BSFV would run into trouble if the ω which has a higher mass than the ρ were the only $T=0$ vector meson (or the only $T=0$, $J=1-$ three-pion resonance).

It is evident that the introduction of a second neutral vector meson with a mass lower than the ρ mass will help remedy this situation. Yet one may still argue that if η^0 is coupled less strongly than ω^0 to $N\bar{N}$, then the η meson effect might not help too much. This, however, is not necessarily the case. It can be shown, using an argument originally given by Gell-Mann and Zachariasen,[4] that if the "universal" coupling constant of η^0 to the hypercharge current defined at $s=0$ does not differ appreciably from the $\eta N\bar{N}$ coupling constant defined at $s=m_\eta{}^2$, then there must be a substantial contribution to the isoscalar charge form factor from the one η state, the crux of the matter here being that both η^0 and the "isoscalar photon" are coupled to the same conserved hypercharge current. Moreover, in a theory which is sufficiently symmetric between N and Ξ, it is easy to show that the transition "isoscalar photon" $\to \omega^0$ must be forbidden to the extent that the $N\Xi$ mass difference could be ignored. (Recall that the baryonic current is even under $N \rightleftarrows \Xi$, while the hypercharge current is odd.)

But let us work backwards, so to speak, and look at the experimental data first. If there are two $T=0$ vector meson states, it is natural to modify the BSFV formula in the following way:

$$F_1^s(q^2) = \frac{\alpha_\eta m_\eta{}^2}{q^2+m_\eta{}^2} + \frac{\alpha_\omega m_\omega{}^2}{q^2+m_\omega{}^2} + (1-\alpha_\eta-\alpha_\omega). \quad (2)$$

Crudely speaking, α_η, α_ω, and $(1-\alpha_\eta-\alpha_\omega)$ represent the fractions of the isoscalar charge contributed by the one η state, the one ω state, and all

other (hopefully very massive) states, respectively. If we regard $m_\eta^2 = 16\, m_\pi^2$ and $m_\omega^2 = 32\, m_\pi^2$ as experimentally determined quantities, the formula contains only two independent adjustable parameters, one of which is more or less determined by the requirement $\langle r_1^2\rangle_p^{1/2} = 0.8\times 10^{-13}$ cm, $\langle r_1^2\rangle_n^{1/2} = 0$. Crude numerical estimates show that the observed data can be adequately reproduced by[19]

$$\alpha_\eta = 1.2, \quad \alpha_\omega = -0.7.$$

On the other hand, for $F_1^V(q^2)$ the original BSFV form suffices so that we have

$$F_1^V(q^2) = \frac{\alpha_\rho m_\rho^2}{q^2 + m_\rho^2} + (1 - \alpha_\rho), \tag{3}$$

just as before; the data require

$$\alpha_\rho = 1.1 - 1.2, \quad m_\rho^2 = 19\, m_\pi^2 - 22\, m_\pi^2.$$

(The slight "discrepancy" between this value for m_ρ^2 and the "observed" value $m_\rho^2 = 29\, m_\pi^2$ is somewhat puzzling.)

Gell-Mann and Zachariasen[4] have noted that if ρ and η are coupled to the conserved isospin and the hypercharge current, respectively, and if the bare masses of ρ and η are infinite (or very large), then the constants α_ρ and α_η are directly related to the form factors of the vector type couplings of the vector mesons to the nucleon at zero momentum transfer, or, equivalently, to the ratios of the "universal" coupling constant $f_\rho^2/4\pi$ or $f_\eta^2/4\pi$ at zero momentum transfer to the "polology" coupling constant measurable at $s = m_\rho^2$, m_η^2 denoted by $f_{\rho N\bar{N}}^2/4\pi$, $f_{\eta N\bar{N}}^2/4\pi$:

$$\alpha_\rho = [1/F_{\rho N\bar{N}}(s)]_{s=0} = f_{\rho N\bar{N}}/f_\rho,$$
$$\alpha_\eta = [1/F_{\eta N\bar{N}}(s)]_{s=0} = f_{\eta N\bar{N}}/f_\eta. \tag{4}$$

It is extremely gratifying that the observed values of α_ρ and α_η are so close to unity. We do not yet understand the deep reason for this, but in view of (4), relations such as $\alpha_\rho \sim 1$ and $\alpha_\eta \sim 1$ seem much more plausible in a theory in which the vector meson states coupled to the conserved currents are introduced in the very beginning, rather than in a theory in which these rather narrow resonant states emerge dynamically, if they do at all, in a mysterious "self-generating" manner à la Chew.[20] Should the α's for other charged particles also turn out to be approximately equal to unity, then, even within the framework of dispersion theory in which all energy momenta are on the mass shell, it would become meaningful to talk about the universal coupling of $\rho(\eta)$ to the particles bearing isospins (hypercharges). Initial steps along this line have already been made in comparing the effect of ρ on πN scattering (proportional to $f_{\rho N\bar{N}} f_{\rho\pi\pi}$) with the width of ρ (proportional to $f_{\rho\pi\pi}^2$).[4,21,22] It appears likely that the notions of universality and conserved vector currents are important elements in our quantitative, as well as qualitative,[1] understanding of the dynamics of strong interactions.

It is a pleasure to thank Professor W. Selove, Professor R. Hofstadter, and especially Dr. P. Schlein for interesting discussions on the experimental aspects of the problem. Thanks are also due to Dr. M. Hamermesh for his hospitality extended to the author at Argonne National Laboratory where the major part of the present work was carried out.

---

*This work was supported by the U. S. Atomic Energy Commission.

[1] J. J. Sakurai, Ann. Phys. 11, 1 (1960). As for the "mass problem" see V. I. Igievetski and I. V. Polubarinov, J. Exptl. Theoret. Phys. 41, 247 (1961) [translation: Soviet Phys.—JETP (to be published)].

[2] J. J. Sakurai, Nuovo cimento 16, 388 (1960).

[3] Private communication from P. Schlein based on work of the Johns Hopkins—Northwestern group. Preliminary data of the group have been reported by A. Pevsner [Proceedings of the International Conference on High-Energy Physics held at Aix-en-Provence, September, 1961 (to be published)].

[4] M. Gell-Mann and F. Zachariasen, Phys. Rev. 124, 953 (1961).

[5] A. R. Erwin, R. March, W. D. Walker, and E. West, Phys. Rev. Letters 6, 628 (1961); E. Pickup, D. K. Robinson, and E. W. Salant, Phys. Rev. Letters 7, 192 (1961). These papers contain more complete references to the earlier papers on this subject.

[6] B. C. Maglić, L. W. Alvarez, A. H. Rosenfeld, and M. L. Stevenson, Phys. Rev. Letters 7, 178 (1961); N. H. Xuong and G. R. Lynch, Phys. Rev. Letters 7, 327 (1961); M. L. Stevenson, G. R. Kalbfleisch, B. C. Maglić, and A. H. Rosenfeld, Phys. Rev. (to be published).

[7] It is amusing that the threshold energy for $\eta + N$ coincides with the energy of an anomalously sharp peak in $\gamma + p \to \pi^+ + n$ observed by L. Hand and C. Schaerf [Phys. Rev. Letters 6, 229 (1961)]. Thus the Hand-Schaerf anomaly could be a cusp effect. Incidentally, contrary to J. S. Ball and W. R. Frazer [Phys. Rev. Letters 7, 204 (1961)], the usual 600-Mev πN resonance cannot possibly be attributed to a threshold effect due to $\pi + N \to \rho + N$ since the ρN threshold is 170 Mev above the 600-Mev resonance. It is possible that the 600-Mev resonance is a bound state of a ρ and an N (bound by the exchange of a ρ), which, however, decays strongly into $\pi + N$, etc. [J. J. Sakurai (to be published)].

[8]E. Teller, in Proceedings of the Sixth Annual Rochester Conference on High-Energy Physics (Interscience Publishers, Inc., New York, 1956), Chap. VII, p. 18. See also Y. Fujii, Progr. Theoret. Phys. (Kyoto) 21, 232 (1959).

[9]G. Breit, Phys. Rev. 120, 287 (1960). See also R. S. McKean, Jr. (to be published).

[10]G. Breit, Proc. Natl. Acad. Sci. U. S. 46, 746 (1960).

[11]Because of an unfortunate historic accident, the nomenclature implied by this identification is contrary to that of Gell-Mann [M. Gell-Mann in his report at the La Jolla Conference on the Theory of Strong and Weak Interactions, June, 1961 (unpublished); also M. Gell-Mann, Phys. Rev. (to be published), and reference 4]. Despite $m_\rho \approx m_\omega$, ρ and ω do not seem to belong to the same octet of the unitary symmetry model. Rather the observed ω is Gell-Mann's B, and our conjectured η is Gell-Mann's ω. Independently of Gell-Mann, A. Salam and J. C. Ward [Nuovo cimento 20, 419 (1961)] and Y. Ne'eman [Nuclear Phys. 26, 222 (1961)] have constructed vector meson theories of strong interactions based on unitary symmetry. Such theories can also accommodate two $T=0$ vector mesons, one belonging to an octet, the other being a singlet all by itself even though Salam and Ward and Ne'eman considered only the one belonging to the octet. In all such models, the postulated symmetries must be badly broken. So far, the only practical advantage of such theories over the original VTSI of reference 1 seems to be the prediction of an $|S|=1$ vector meson, which might be identified with K^* of M. H. Alston, L. W. Alvarez, P. Eberhard, M. L. Good, W. Graziano, H. K. Ticho, and S. G. Wojcicki [Phys. Rev. Letters 6, 300 (1961)]. If the Y_1^* spin is $\frac{3}{2}$, and the $\Lambda\Sigma$ parity is even, then the observed very small Σ/Λ branching ratio for Y_1^* may fit nicely with Gell-Mann's "eightfold way" (but not the unitary symmetry model based on the Sakata triplet) which requires $f_{\pi\Sigma\Sigma}{}^2=0$ with "D-type" meson-baryon couplings. See, e.g., J. Franklin (to be published). Note also that Franklin's choice $f_{\pi\Lambda\Sigma}{}^2 \gg f_{\pi\Sigma\Sigma}{}^2 \approx 0$ can accommodate Y_0^*, Y_1^*, and Z^* ($T=2$) as $p_{3/2}$ pion-hyperon resonances belonging to a "representation 27" of the "eightfold way." (Recall that $8\times 8=1+8+8+10+10=27$.)

[12]G. F. Chew and S. C. Frautschi, Phys. Rev. Letters 5, 580 (1960); Phys. Rev. 123, 1478 (1961).

[13]R. Hofstadter and R. Herman, Phys. Rev. Letters 6, 293 (1961); R. M. Littauer, H. F. Schopper, and R. R. Wilson, Phys. Rev. Letters 7, 144 (1961). According to R. Hofstadter (private communication), more reliable data will become available in the near future.

[14]E. Clementel and C. Villi, Nuovo cimento 4, 1207 (1958).

[15]S. Bergia, A. Stanghellini, S. Fubini, and C. Villi, Phys. Rev. Letters 6, 367 (1961).

[16]Y. Nambu, Phys. Rev. 106, 1366 (1957).

[17]W. R. Frazer and J. R. Fulco, Phys. Rev. 117, 1609 (1960). See also S. D. Drell, in Proceedings of the 1958 Annual International Conference on High-Energy Physics at CERN (CERN, Geneva, 1958), p. 27, and a remark made by M. Gell-Mann after Drell's talk (p. 33, loc. cit.).

[18]G. F. Chew, Phys. Rev. Letters 4, 142 (1960). However, Chew's "dynamical" approach to the three-pion resonance, in which each pair of pions resonate in $T=1$, $J=1$, faces several difficulties which will be discussed elsewhere.

[19]We would like to emphasize the preliminary nature of these numbers. A more detailed analysis using Eq. (2) is now in progress by R. Hofstadter and collaborators using their new data.

[20]It is true that even in the approach of Chew and others $\alpha_\rho=\alpha_\eta=1$ would follow if the ρ state and the η state completely dominated the unsubtracted dispersion representations for the charge form factors. The narrow widths of ρ and η, however, suggest that these states are relatively weakly coupled to pions; thus the dominance of ρ and η would be rather surprising in Chew's "dynamical" approach.

[21]J. J. Sakurai, Bull. Am. Phys. Soc. 5, 414(T) (1960); Enrico Fermi Institute of Nuclear Studies Report EFINS-60-63 (unpublished).

[22]In the La Jolla Conference, June, 1961, the author reported that the universality hypothesis requires the ρ width to be about 170 Mev (in agreement with the information on the ρ width available at that time[5]) provided that the parameter C_1 of Bowcock, Cottingham, and Lurié (which essentially measures the effect of the ρ contribution on πN scattering, and is proportional to $f_{\rho\pi\pi}f_{\rho N\bar{N}}$ of the vector meson approach) has been correctly evaluated in J. Bowcock, W. N. Cottingham, and D. Lurié [Phys. Rev. Letters 5, 386 (1960)]. At that time M. Cini remarked that more detailed calculations by G. Höhler and collaborators have shown that the BCL value for C_1 must be reduced by a factor of 2 or 3. Meanwhile, the more recent $p\bar{p}$ experiments of Maglić et al.[6] and Stevenson et al.[6] suggest that the ρ width is probably as small as 80 Mev. Thus the universality hypothesis seems to be valid again.

EXPERIMENTAL TESTS OF MACH'S PRINCIPLE*

R. H. Dicke
Palmer Physical Laboratory, Princeton University, Princeton, New Jersey

(Received September 11, 1961)

In this note it will be shown that, contrary to the suggestion of Cocconi and Salpeter,[1] the extremely precise null result of the experiments of Hughes, Robinson, and Beltrow-Lopez[2] and Drever[3] is to be expected, resulting from an application of Mach's principle.

According to Mach's principle, as formulated by Bishop Berkeley,[4] Mach,[5] and Sciama,[6] the inertial forces experienced in an accelerated laboratory are gravitational, having their origin in the distant matter of the universe, accelerated relative to the laboratory. Because of the tensor character of the gravitational-inertial field, it should exhibit tensor polarization properties. In particular, as suggested by Cocconi and Salpeter, because of the flattened rotating mass distribution of our galaxy, the inertial reaction having its origin in this mass distribution should exhibit some spatial anisotropy. This should appear in the formalism as a tensor inertial mass. Cocconi and Salpeter suggested that if Mach's principle were valid, the effects of this tensor inertial mass would appear as a spatial anisotropy in certain experiments. Several experiments, designed to test Mach's principle in this way, have been performed or analyzed.[1-3,7] By far the most accurate has been that of Drever.[3]

It will be shown that the experiments do not represent a test of Mach's principle in the manner suggested by Cocconi and Salpeter. On the contrary, and in agreement with the requirements of Mach's principle, the experiments show that, with great precision, the anisotropy of the inertial mass is universal, the same for all particles.

Expressed relativistically, the suggestion of Cocconi and Salpeter[1] is that the four-momentum of a particle can be written as

$$P_i = m_{ij} u^j, \tag{1}$$

where u^i is the four-velocity of the particle. In the absence of a gravitational field, the particle is assumed to obey the equations of motion,

$$dP_i/ds = F_i, \tag{2}$$

where F_i is the four-force acting on the particle and as usual F_i satisfies the condition

$$F_i u^i = 0. \tag{3}$$

As Mach's principle associates the inertial reaction with the matter distribution in the universe, an anisotropy in the inertial mass should be universal, the same for all particles at the same space-time location, for all particles would see the same mass distribution. With the assumption that the inertial reaction is universal, the tensor m_{ij} can be expressed as

$$m_{ij} = m f_{ij}, \tag{4}$$

where f_{ij} is a universal tensor field (dimensionless).

A serious objection to Eqs. (1)-(4) can be raised. Equations (2) and (3) are generally not consistent with the constraint condition,

$$g_{ij} u^i u^i = u^i u_i = 1. \tag{5}$$

Consistent equations can be obtained from a variational principle. We note that to generate a momentum such as Eq. (1), linear in a four-velocity, a first condition to be satisfied is that the Lagrangian of the particle should be a function of the invariant

$$(d\bar{s}/ds)^2 = f_{ij} u^i u^j. \tag{6}$$

Equations of motion of a free particle (gravitational forces only) are obtained from the variational principle,

$$0 = \delta \int L ds, \tag{7}$$

where variations of the coordinates are to be taken subject to the constraint, Eq. (5). With the assumption that f_{ij} and g_{ij} are not equivalent, the resulting expression for the four-momentum is linear in some four-velocity only for the unique choice,

$$L = m(f_{ij} u^i u^j)^{1/2}. \tag{8}$$

With this choice, the constraint condition, Eq. (5), is satisfied by the equations of motion automatically, without introducing the condition of constraint in the variational calculation. As a result, the equations of motion do not contain g_{ij} explicitly.

Substituting Eq. (8) in Eq. (7), the equations of

motion of a free particle are

$$\frac{d}{ds}\frac{m_{ij}u^j}{(f_{ki}u^k u^j)^{1/2}} - \tfrac{1}{2}\frac{m_{jk,i}u^j u^k}{(f_{kj}u^k u^j)^{1/2}} = 0. \qquad (9)$$

These are most conveniently expressed, introducing f_{ij} as a new metric tensor, by defining

$$d\bar{s}^2 = f_{ij}dx^i dx^j, \qquad (10)$$

$$\bar{u}^i = dx^i/d\bar{s}. \qquad (11)$$

With these substitutions, Eq. (9) becomes

$$\frac{d}{d\bar{s}}(m_{ij}\bar{u}^j) - \tfrac{1}{2}m_{jk,i}\bar{u}^j\bar{u}^k = 0. \qquad (12)$$

The resulting particle trajectories are geodesics of the new geometry, with f_{ij} as metric tensor. The limiting trajectories of particles with infinite energy are null geodesics of the new geometry.

Inasmuch as g_{ij} does not appear explicitly in the classical equations of motion of a particle, the appropriate quantum mechanical wave equations, giving equations of motion of expectation values equivalent to the classical equations, are constructed by employing f_{ij} as the metric tensor. For example, the appropriate Lagrangian density for the Klein-Gordon wave function is

$$\tfrac{1}{2}\hbar^2 f^{ij}\varphi_{,i}\varphi_{,j} - \tfrac{1}{2}m^2\varphi^2. \qquad (13)$$

It may be noted with the assumption made above, that the inertial reaction is universal, the same for all particles including photons and pions, the metric tensor g_{ij} appears nowhere in the formalism. In fact, for the geometry defined by measurements in the usual way with real rods and clocks, f_{ij} is the metric tensor.[8]

It should be noted also, that because of the universal character of the inertial anisotropy, being present in the same way for all particles (or fields), the spatial anisotropy is unobservable locally. The easiest way to see this is to note that a coordinate system can always be chosen in such a way as to cause f_{ij} to be locally Minkowskian with vanishing first derivatives. For this coordinate system, the anisotropy of inertial mass appears explicitly nowhere in the equations.

While, with these assumptions, inertial anisotropy is not locally observable, the fact that the geometry defined by real rods and clocks is non-Euclidean may be interpreted as due in part to the effect on rods and clocks of the anisotropy of the inertial mass of the elementary particles which comprise the rods and clocks.

It is concluded finally that the extremely accurate null result of the experiment of Hughes et al. does not cast doubt upon the validity of Mach's principle. On the contrary, and in accordance with the requirements of Mach's principle, this important experiment shows, with great precision, that inertial anisotropy effects are universal, the same for all particles.

---

*This research was supported in part by the Office of Naval Research, the U. S. Atomic Energy Commission, and the Higgins Scientific Trust Fund.

[1]G. Cocconi and E. E. Salpeter, Nuovo cimento 10, 646 (1958); Phys. Rev. Letters 4, 176 (1960).

[2]V. W. Hughes, H. G. Robinson, and V. Beltrow-Lopez, Phys. Rev. Letters 4, 342 (1960).

[3]R. W. P. Drever, Phil. Mag. 6, 683 (1961).

[4]G. Berkeley, The Principle of Human Knowledge (1710), par. 111-117.

[5]E. Mach, Conservation of Energy (1872) (edition of Open Court Publishing Company, Chicago, Illinois, 1911), Note No. 1; Science of Mechanics (1883) (edition of Open Court Publishing Company, Chicago, Illinois, 1902), Chap. II, Sec. VI.

[6]D. W. Sciama, Monthly Notices Roy. Astron. Soc. 113, 34 (1953); The Unity of the Universe (Doubleday, New York, 1959), Chaps. 7-9.

[7]C. W. Sherwin, H. Frauenfelder, E. L. Garwin, E. Lüscher, S. Margulies, and R. N. Peacock, Phys. Rev. Letters 4, 399 (1960).

[8]What then is the significance of the redundant tensor g_{ij}? As was discussed recently [C. Brans and R. H. Dicke, Phys. Rev. 124, 925 (1961)], the choice of units of length and time are arbitrary and physical laws must be invariant under position-dependent transformation of units. As a result, considerable freedom in the definition of the metric tensor exists. While f_{ij} would be the natural and simplest choice, the metric tensor can be modified at will and can be defined as g_{ij} by the appropriate redefinition of units. In particular, there exist definitions of units for which the space is flat, all the Riemannian invariants being zero.

ERRATA

K_2^0 DECAYS AND INTERACTIONS. D. Luers, I. S. Mittra, W. J. Willis, and S. S. Yamamoto [Phys. Rev. Letters 7, 255 (1961)].

On page 257, the first line at the top of the page reads: "Using the $\Delta I = \frac{1}{2}$ rule, he predicts $a = -0.0109 \pm 0.022$. We find $a = 0.0171 \pm 0.0065$." It should read: "We find $a = -0.0171 \pm 0.0065$."

FIRST-ORDER TERRESTRIAL ETHER DRIFT USING THE MÖSSBAUER RADIATION. Martin Ruderfer [Phys. Rev. Letters 5, 191 (1960)].

The theory of the proposed experiment is incomplete because the first-order variation of frequency with motion is not considered. In the Fitzgerald-Lorentz contraction theory, the frequency of a moving clock is $f_0(1 - w^2/c^2)^{1/2}$, where f_0 is the frequency when the clock is at rest in the ether and w is its velocity through the ether. For the radiator at the center of the turntable, $w = v$ and the frequency, f, of the radiator is

$$f = f_0(1 - v^2/c^2)^{1/2}.$$

For the absorber, $w = |\vec{v} + \vec{\omega}_S|$ and the frequency, f_a, of the absorber is

$$f_a = f_0[1 - (\omega^2 s^2 + v^2 - 2\omega s v \sin\theta)/c^2]^{1/2}.$$

The relative frequency shift due to clock motion is, to first order,

$$|\Delta f/f|_{cl} = (f_a - f)/f = \omega s v \sin\theta/c^2.$$

It is readily verified that this is also obtained when the radiator is not at the center of the turntable. This frequency shift is equal to the frequency shift found due to phase shift in rotation. The contraction theory therefore predicts a null effect as does relativity theory for a one-way rotating terrestrial ether drift experiment. The proposed experiment is not a crucial experiment for deciding between the two theories. To conform to both theories, the proper interpretation of the predicted null result is that detection of an ether is precluded as required by the special theory of relativity and that existence of an ether is permitted as required by the contraction theory.